*Republic of Iraq*

*Ministry of Higher Education*

*And Scientific Research*

*University of Babylon*

*College of Engineering*

*Department of Mechanical Engineering*

# *Simulation Study of Temperature Distribution on Cutting Tools with Effect of Cutting Process Parameters*

*A Thesis*

***Submitted to the College of Engineering / University of Babylon in Partial Fulfillment of the Requirements a ward of Degree of Master in Engineering / Mechanical Engineering / Power***

*By*

***Haneen Hazim Abdu Aali Hassan***

***Supervised By***

***Assist Prof. Dr. Abdul Kareem Jalil Kadhim***

***And***

***Assist Prof. Dr. Samir Mohammed Abdul Haleem***

***2022 A.D*** ***1443 A.H***

# بسم الله الرحمن الرحيم

{ قالوا سبحانك لا علم لنا إلأ ما علمتنا أنك أنت العليم الحكيم}

سورة البقرة

الآية (32)

***صدق الله العظيم***

# *Certification*

I certify that the preparation of this thesis, entitled " ***Simulation Study of Temperature Distribution on Cutting Tools with Effect of Cutting Process Parameters***" was prepared by***"Haneen Hazim Abdul Aali"*** under my supervision at the Department of mechanical Engineering, College of Engineering, University of Babylon, as a partial fulfillment of the requirements for the degree of Master of Science in Mechanical Engineering (power).

**Signature:**

***Assist Prof. Dr. Abdul Kareem Jalil Kadhim***

**(First supervisor)**

**/ /2022**

**Signature:**

***Assist Prof. Dr. Samer Mohammed Abdul Haleem***

**(Second supervisor)**

**/ /2022**

# DEDICATION

*Dedicate My Thesis to*

***My Family***

***And specially my husband*** ***Ali***

***My mother***

***My brother*** ***Haider***

*Who always encouraged and supported me, and without them this work would not have been possible.*

***Haneen 2022***

# *Acknowledgements*

*(In The Name of Allah, The Gracious, The Merciful)*

*(Thanks to Allah for his guidance and help)*

*I wish to express my sincere thanks and deep gratitude to my supervisors* ***Assist Prof. Dr. Samer Mohammed Abdulhaleem*** ***and*** ***Assist Prof. Dr. Abdul Kareem Jalil Kadhim*** *and for their invaluable help, advice and encouragement during the various stages of the present work.*

*I would like to express my gratitude to the head of the department for guidance and support.*

*My deepest thanks, love and gratitude for all of* ***my family****. This study would not have been completed without their love and continuous support.*

*Haneen 2022*

# ABSTRACT

To improve the productivity of a machining operation, the thermal field must be determined. The most of the power used to cut the metal during shaping process was transformed into heat. This thesis presents numerically the influence of cutting parameters on the temperature distribution in shaping process by using Finite element method and Finite volume method based on ANSYS 2020R2 software. Temperature at tool-chip interface is determined by using Explicit Dynamic, it considers as boundary condition in one side of insert. The effects of heat transfer and heat flux on cutting tools with materials of High speed steel, Carbide, Ceramic are investigated numerically by ANSYS fluent software. The numerical model was validated with the previous study. The workpiece model is created with materials of Aluminium, Iron, Copper, and it designed as rectangular with a length, height and width of (150 mm, 50 mm and 30mm) respectively. The cutting parameters are selected with three cutting speeds (6, 8, and 10) m/s, with three depth of cut (1.5, 2, and 2.5) mm. For all simulations, the rake angle is fixed at ($6^{o}$). The results show that the temperature at the tip (tool-work piece contact area) is the highest and gradually decreases towards the surface, and that most generation of temperature is produced from the cutting speed parameter when compared with that produced from the cutting depth parameter, Also results show that High speed steel and Carbide have a temperature less than the Ceramic ($Al_2O_3$) so that the productivity will increase with the High speed steel and Carbide materials utilizing as cutting tool. The maximum temperature for High speed steel is 537.14 K while the Carbide and Ceramic achieved 578.87 K, 648.3 K respectively. The lowest and maximum temperature was measured at a cutting speed of 6 m/s and 10 m/s, respectively.

The optimum cutting condition has been obtained with High speed steel cutting tool material at 6 m/s cutting speed and 1.5 mm cutting depth.

# *Table Of Contents*

## Nomenclatures

| Symbol | Description | Unit |
|---|---|---|
| $C_p$ | Specific heat capacity | J/Kg.K |
| $F_f$ | frictional force along the interface | - |
| $h$ | Heat transfer coefficient for the tool–work-piece interface | (W/m$^2$.k) |
| H | contact length | mm |
| k | Thermal conductivity | W/m.K |
| $\dot{q}$ | heat generation per unit volume | W/m$^3$ |
| $\bar{\bar{q}}_c$ | Heat conduction flux density at the tool–workpiece interface | W/m$^3$ |
| $\bar{\bar{q}}_f$ | frictional heat generation rate per unit area | W/m$^2$ |
| $\dot{q}_p$ | Heat generated per unit volume due to plastic work | W/m$^3$ |
| $\bar{\bar{q}}_{\rightarrow tool}$ | Heat flux density in the tool at the tool–workpiece interface | W/m$^2$ |
| $\bar{\bar{q}}_{\rightarrow workpeice}$ | Heat flux density in the workpiece at the tool–workpiece interface | W/m$^2$ |
| $T_w, T_t$ | Temperatures, respectively, of workpiece and tool at the tool–workpiece interface | $^0$C |
| t | Undeformed chip thickness | mm |
| $t_p$ | plastic zone thickness | mm |
| $t^2$ | chip thickness | mm |
| $V_s$ | sliding velocity | m/s |
| $w_1$ | width of cut | mm |

| Greek Symbols | | |
|---|---|---|
| **Symbol** | **Description** | **Unit** |
| $\boldsymbol{\mu}$ | Constant coefficient of friction | - |
| $\boldsymbol{\eta_f}$ | Frictional work conversion factor | - |
| $\boldsymbol{\beta}$ | Heat generation coefficient (fraction of the friction energy generated in the tool side) | - |
| $\rho$ | Material density | $Kg/m^3$ |
| $\dot{\boldsymbol{\gamma}}$ | Maximum shear strain rate | 1/s |
| $\boldsymbol{\sigma_n}$ | Normal friction stress | MPa |
| $\boldsymbol{\eta_p}$ | Plastic work conversion factor (Taylor-Quinney factor) | - |
| $\boldsymbol{\alpha}$ | Rake angle | degree |
| $\boldsymbol{\delta}$ | ratio of thickness of secondary zone to the chip thickness | - |
| $\boldsymbol{\tau_{fr}}$ | Shear friction stress | MPa |
| $\boldsymbol{\tau}$ | Shear stress | MPa |
| $\boldsymbol{\tau_x}$ | Shear stress at a distance x from the tool edge | MPa |
| $\bar{\tau}_{max}$ | Shear stress limit | MPa |
| $\boldsymbol{\sigma}$ | Uniaxial stress | MPa |
| $\dot{\boldsymbol{\varepsilon}}$ | Uniaxial strain rate | 1/s |
| $\bar{\boldsymbol{\sigma}}_{\boldsymbol{s}}$ | Von-Mises equivalent stress | MPa |
| $\dot{\boldsymbol{\varepsilon}}_{\boldsymbol{p}}$ | Von-Mises equivalent plastic strain-rate | - |

## ABBREVIATIONS

| Abbreviation | Description |
|---|---|
| **B.C** | Boundary Condition |
| **CAE** | Cathodic Arc Evaporation |
| **CFD** | Computational Fluid Dynamics |
| **DOC** | Depth of cut |
| **emf** | Electro motive force |
| **FDM** | Finite Difference Method |
| **FEM** | Finite Element Method |
| **FVM** | Finite Volume Method |
| **HSS** | High Speed Steel |
| **PVD** | Physically Vapor Deposited |
| **SEM** | Scanning electron microscope |

# CHAPTER ONE

# INTRODUCTION

# CHAPTER ONE

# Introduction

## 1.1 General

The metal cutting processes are widely used to remove unwanted material, to achieve dimensional accuracy and desired surface finish of engineering components. In metal cutting processes, the unwanted material is removed by the cutting tool in the form of chips when passed away on the blank or stock. In case of conventional machining, the cutting tool is significantly harder than the work piece. However, cutting tool fail by plastic deformation, wear out or mechanical breakage**[1]**.

Large amounts of energy are needed for any machining on metal and alloy when plastic deformation is related to the formation of chips; this energy is then transformed to heat, which ultimately raises the cutting zone temperature. This is a major problem for both the cutting tool's effectiveness and the quality of the finished product. Temperatures in the cutting area are affected by the length of contact between the tool and the chip, as well as cutting forces and friction between the tool and the workpiece material. A large proportion of heat created during machining is transmitted to the cutting tool and workpiece, while the remaining is dissipated with the chip. As a result, the cutting condition, tool performance, and tool life are all affected by the contact length between the tool and the chip**[2]**. In order to examine the impact of the tool edge geometry and cutting parameters on the surface quality, especially on the machining generated stresses, advanced process simulation

approaches are required. The goal of this work is to use a suitable numerical method to study the temperature distribution on a cutting tool made of different materials at varied machining variables.

## 1.2 Types of Cutting Processes

Metal cutting mechanics analysis employs two types of cutting: Cutting orthogonally and obliquely. In orthogonal cutting, when a cutting edge that is perpendicular to the direction of relative motion between the tool and the work piece, unnecessary material is removed from the work piece. Since the material removal process is considered to be uniform along the cutting edge in orthogonal cutting, it is a two-dimensional plane strain problem. In oblique cutting, the principal cutting edge is inclined to the direction of the cutting velocity by an inclination angle. As shown in Fig. (1-1)**[3]**.

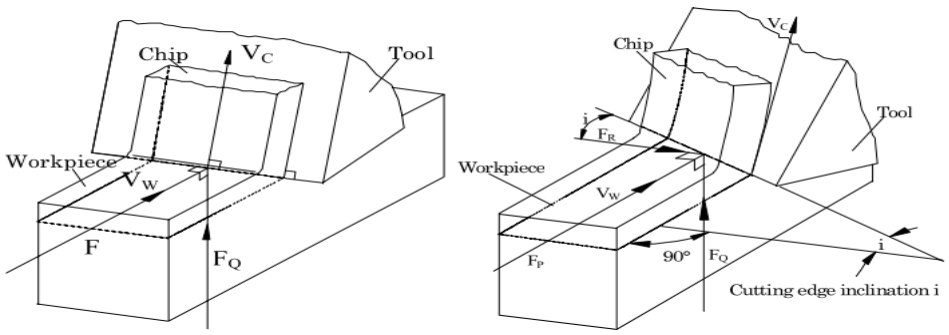


(a) (b)

Figure (1-1). Types of cutting (a) Orthogonal cutting (b) Oblique cutting**[3]**

## 1.3 Zones of Heat Generation on Shaping process

In the cutting process, there are three deformation zones. As shown in Fig. (1-2). The metal chip is sheared in the main plastic deformation zone, moves on the rake face due to sticking and sliding friction in the secondary zone, and the final surface touches the tool's flank face in the third deformation region. Cutting generates heat to be developed in all three

regions, which increases the temperature of the work material and cutting tool **[4]**.

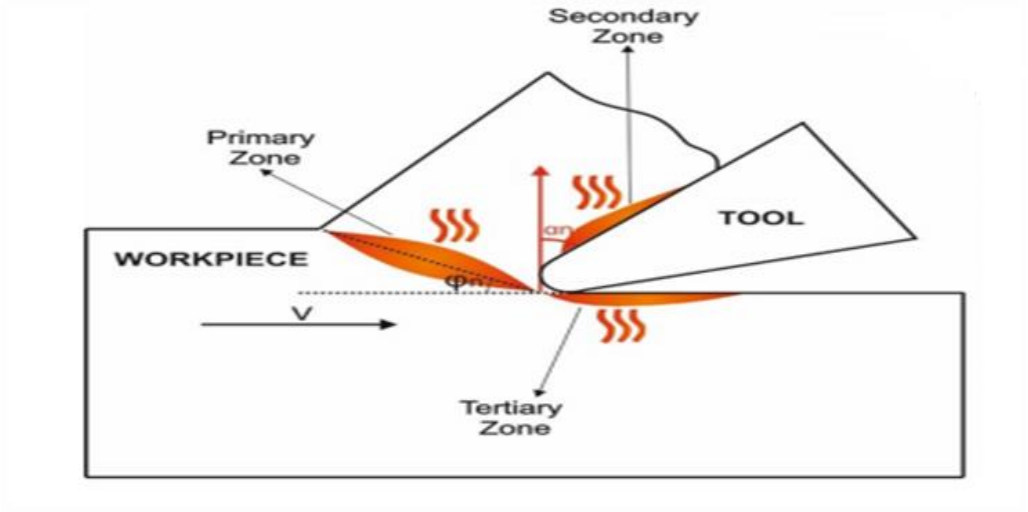


Figure (1-2). Deformation zones in metal cutting **[4]**

## 1.4 Techniques for temperature measurement

### 1.4.1 Thermocouples

It is formed between tool and work piece. The hot end of the tool and the cold end of the work piece operate as thermocouples, producing an emf proportional to the temperature differential. The chuck and tailstock center are isolated from the work piece. The work piece's end is attached to a copper wire that has been immersed in a mercury cup and serves as a freezing end. This point and tool connector offer output for connecting to a mille voltmeter. Laboratory procedures can be used to produce a calibration curve between tool temperature and emf **[5].**

### 1.4.2 Thermocouples embedded

The thermocouples are implanted in small holes eroded in HSS tool from the bottom face up to a preset distance from the rake face, allowing temperature measurement at multiple places along the tool's rake face.

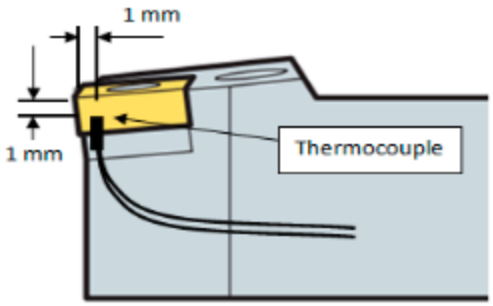


Figure (1-3): Position of thermocouple**[6].**

### 1.4.3 Photographic Technique Using Infrared

This method involves capturing images of the side face of a tool-chip as it is being cut and comparing them to strips of known temperature.

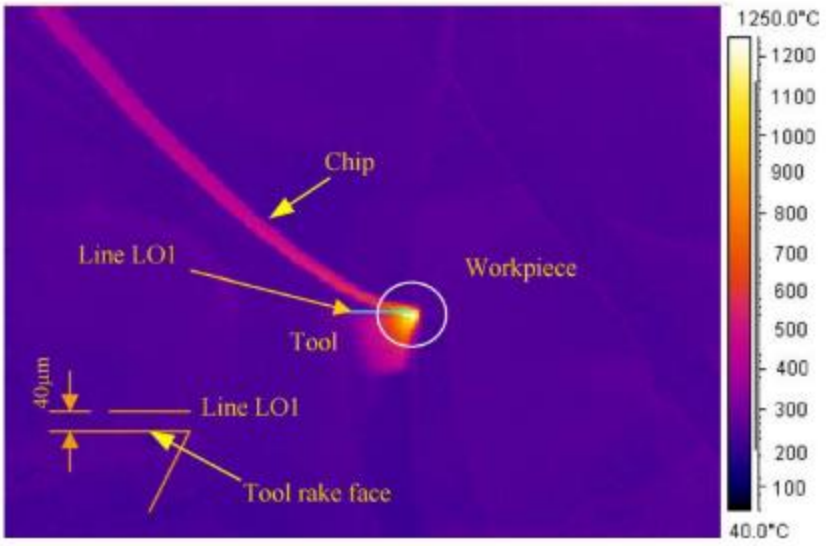


Figure (1-4): Infrared photograph of the cutting process**[7].**

## 1.5 Factors Affecting Cutting Temperature

The many variables that influence to the tool temperature have an impact on the size of the shear zone and chip tool contact length, and hence the region across which heat is diffused. A shorter duration of contact

between the chip and the tool causes a significant temperature increase. The following things influence cutting temperature**[8]:**

### 1.5.1 Work Piece and Tool Material

The tensile strength and hardness of the work piece material have a significant impact on cutting temperature. When a material has a high tensile strength and hardness, it requires more energy to make chips and generates more heat. Higher thermal conductivity cutting tools materials yield lower temperatures than lower thermal conductivity cutting tools.

### 1.5.2 Cutting Conditions

The cutting speed has predominant effect on the cutting temperature. Feed has little effect and depth of cut the least. The higher the cutting speed the faster the surface feed that the tool travels, the more heat will be generated by friction. The higher feed rate as well as depth of cut results in more material being removed, which result in higher friction.

### 1.5.3 Cutting Fluid

At very high speeds, the cutting fluid cannot reach the tool-chip interface and has no effect on the tool-chip interface temperature. The fluid is transported away more quickly by the outward flowing chip than it could be pressed between the tool and the chip.

### 1.5.4 Tool Geometry

The temperature is affected by the rake angle. Temperature variations of 20 °C have only been seen for rake angle changes ranging from -10° to +30°. It rises as the approach angle and radius of the tool increase.

## 1.6 Variables of Cutting Process

Figure (1.3) shows orthogonal cutting and tool geometry variables. (t) It is the undeformed chip thickness, often known as the depth of cut. The chip thickness is denoted by tc. The rake face is the face where the chip and tool come into contact. The rake angle (α) is the angle formed by the rake face

and the freshly machined surface normal. The clearance face is the surface over which the machined surface travels. The clearance angle (γ) is the angle formed by the newly machined surface and the clearance face. These factors are significant because they influence the process's features **[3].**

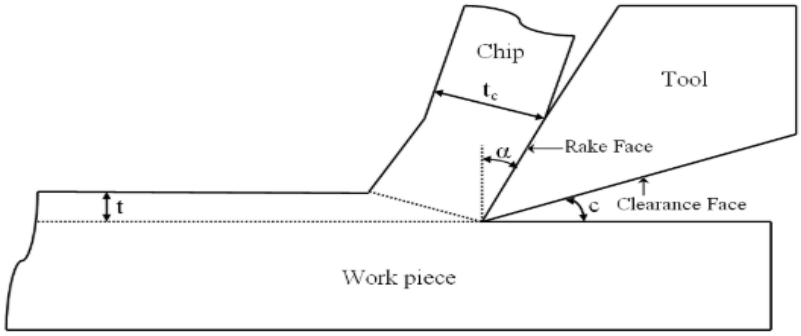


Figure (1-5). Variables in orthogonal cutting **[3]**

## 1.7 Aim and Objectives of the Study

The current study's aim is to successfully *study three-dimensional thermal models of machining processes for a given tool-workpiece material*. The study involves investigation of thermal and mechanical properties, tool geometry, and cutting parameters like speed and depth. To determine the temperature distribution in the cutting tool, a numerical solution is used to predict the tool-chip interface temperature using the finite element approach and the finite volume method. Thus the main objectives of this project are as follows:

1. Numerical solution of the governing equation by using a suitable numerical method.
2. Study the effects of cutting parameters such cutting speed, depth of cuts on tool-chip interface temperature and then use this temperature as constant heat flux that effect on the cutting tool.

3. Study the effect of different materials used for cutting tool such as HSS, carbides, Ceramic.
4. Studying the effect of tool material on the thermal behavior of tool.

## 1.8 Layout of Thesis

The thesis consists of five chapters organized as follows:

1. Chapter One: included an introduction to the importance and types of the metal cutting operation as well as explaining the main areas of heat generation in machining operation.
2. Chapter Two: gives a theoretical and experimental methods to studying the temperature distributions in metal cutting operation.
3. Chapter Three: explain the modeling of the metal cutting and the solution procedure using ANSYS 2020R2 software.
4. Chapter Four: Present results obtained in this work (temperature distributions in metal cutting operation) and their discussion.
5. Chapter Five: Present a conclusions of this work and some recommendations for future work are given in that chapter as well.

# CHAPTER TWO

# LITERATURE REVIEW

# CHAPTER TWO

# LITERATURE REVIEW

A number of mathematical models of cutting process have been published in the literatures. These models have been investigated widely by using a variety of analytical, numerical and experimental techniques. The review made here in is classified in to theoretical and experimental methods.

## 2.1 Theoretical Methods

These methods include the analytical and numerical methods uses to solve the temperature distribution for different machining process and different boundary conditions.

**(Jen et al., 2001)[9]** used a control volume approach used with temperature dependent thermal properties to investigate the temperatures of interrupted cutting tools. For the cases with temperature-dependent thermal characteristics, a transient non-linear three-dimensional numerical analysis was performed. The study was compared to the linear solution with constant thermal characteristics. It was concluded that the:

(a) A good resolution of the mesh size at the tool-chip interface was required to achieve reliable results on temperature distribution in the tool insert.

(b) The conductivity of high-speed steel as a tool insert material was a significant function of tool temperature. The thermal conductivity of the tool reduced as its temperature rose.

(c) The heat flux distribution patterns on the tool-chip interface had a considerable influence on the maximum temperature magnitude.

(d) When the heat flux distribution deviated from the uniform heat flux input profile for the same amount of total energy input, the maximum temperature rose greatly.

**(Majumdar et al., 2005)[10]** developed a method to determine the temperature distribution in a metal cutting process by using a finite element method. The model based on a multi-dimensional steady-state heat diffusion equation, as well as heat lossed at the surfaces due to convection film coefficients. The results showed a rise in tool temperature with increased cutting speed. When machining high carbon steel, the maximum temperature in the tool raised from 709.36 K to 1320 K as the cutting speed increased from 29.6 m/min to 155.4 m/min.

**(Carvalho et al., 2006)[11]** proposed a method to estimate the temperature and the heat flux at the chip–tool interface using the inverse heat conduction problem technique. The thermal model has been obtained by a numerical solution of the transient three-dimensional heat diffusion equation that considerd both the tool and the tool holder assembly. To determine the solution equation the finite volume method has been used. Changing in the thermal properties with the temperature and heat losses by convection have been also considered. Several cutting tests using cemented carbide tools have been performed in order to check the model and to verify the influence of the cutting parameters on the temperature field.

**(Abukhshim et al., 2006)[7]** reviewed previous research's on heat generation and heat dissipation in the orthogonal machining process. In addition, temperature measurement techniques applied in metal cutting have been briefly reviewed. The emphasis was on the comparability of test

results, as well as, the relevance of temperature measurement method to high speed cutting. New temperature measurement results obtained by a thermal imaging camera in high speed cutting of high strength alloys also presented. The research also included an exploration of the different simplifying assumptions related to the geometry of the process components, material properties, boundary conditions and heat partition. The paper proposed some modelling requirements for computer simulation of high speed machining processes.

**(Grzesik, 2006)[12]** determined the temperature distribution in the cutting zone by integrating thermal analytical and simulation models of orthogonal cutting process with uncoated and coated carbide tools. Primarily, 2D FEM simulations were run to provide numerical solutions of temperatures occurring at different points through the chip/tool contact region and the coating/substrate boundary under defined cutting conditions. In addition, an analytical model for heat transfer in the cutting tool was carried out. The changes of the temperature distribution fields resulting from varying heat flux transfer conditions were the main findings of the FEM simulations. Finally, the analytically and numerically predicted average temperatures were validated against the tool-work thermocouple-based measurements .It has been shown that the outcomes of the FEM and analytical models provide quite satisfactory and physically supported results, for both uncoated and three-layer coated tools, concerning values and distributions of cutting temperatures. However, a better accuracy probably has been obtained by tuning friction parameter and heat partition to coated tools with real thicknesses.

**(S. Zhang et al., 2008)[13]** developed an analytical model with constant temperature at tool and chip interface of one-dimensional heat transfer in

monolayer coated tools to investigate temperature distribution in metal cutting. The explicit form of temperature formula were obtained by using the Laplace Transform technique and a Taylor series expansion. Calculations conducted for tools of three coatings (TiN, TiC and $Al_2O_3$) and two substrates (K10 and P10). The transient temperature distributions have shown that the thermo physical parameters of coating and substrate materials have huge influences on temperature distributions in monolayer coated tools. The analytical solution method had demonstrated that $Al_2O_3$ coating has more effective thermal barrier effect than the other two coating materials. The coating thickness also had some influence on temperature distributions in coated tools.

**(Kadirgama et al., 2009)[14]** studied numerically and experimentally the machining process to find the temperature distribution on the cutting tool. They found the effect of feed rate, cutting speed, and axial depth on the temperature distribution. Box-Bennken design method used to select the experiment conditions. Coolant effect on temperature also investigated. The results showed that optimum value of cutting process with $90^0$ with coolant was at speed 100 m/min, depth 1mm, and feed rate 0.1mm/rev. for cutting process with $70^0$ holder with coolant the optimum conditions was at speed 25 m/min, depth 0.5417 m, and feed rate 0.1mm/rev.

**(Kilicaslan, 2009)[3]** used finite element method for modeling and simulation of orthogonal metal cutting. For that purpose, orthogonal cutting simulations of AISI 1045 steel have been performed. At first step, effects of work piece flow stress and friction models on cutting variables such as cutting forces, chip geometry and temperature have been investigated by comparing simulation results with experimental results available in the literature. Then, mechanical and thermal analyses have been performed.

Lastly, effects of rake angle and tool tip radius on strain, temperature and stress distributions have been investigated.

**(Ulutan et al., 2009)[15]** determined the three-dimensional temperature fields on the chip, tool and workpiece during machining by using finite difference method (FDM). The simulations were in acceptable agreement with measurements, although under predicting 20–60 ◦C for low feed rate values. That was mostly due to the fact that for low temperatures (temperatures closer to room temperature), thermal conductivity and density of materials change, affected Reynolds number of the process and thus heat convection coefficient.

**(Yanda et al., 2010)[16]** simulated a three-dimensional orthogonal cutting operations using FEM software (deform-3D) to study the effects of rake angle on the cutting force, effective stress, strain and temperature on the edge of carbide cutting tool. The analysis of results showed that, the increase in the rake angle from negative to positive angle, caused the decrease in cutting force, effective stress and total Von Misses strain. The minimum of the cutting force, effective stress and total Von Misses strain were obtained at rake angle of +15 deg. Increasing the rake caused higher temperature generated on the edge of carbide cutting tool and resulted in bigger contact area between the clearance face and the workpeice, consequently caused more friction and wear.

**(Kisku, 2011)[17]** studied heat influencing the effect of coated and uncoated cemented carbide cutting tool. The solution obtained showed that the temperature at the tip (tool-work piece contact area) was maximum and it went on decreasing towards the surface and it was also observed that the temperature generated for coated tool is little less in comparison to

uncoated cemented carbide insert which showed that the tool life increased by placing a coating layer of TiN (Titanium Nitride).

**(Saragi, 2012)[18]** studied the effect of the temperature distribution on tool life and wear using finite element method by modeling the heat intensity at the cutting zone and shear zone as non-uniform. The work tried to obtain temperature distribution in deformation zones and the temperature increased on the chip side and tool side along the interface. X, Y, Z dimensional (3D) study heat transfer FEA problem was given boundary conditions that specified temperature, insulated and active conditions. The numerical methodology used here is a solid works simulation. Finite element method was used to model the effect of base insulated and base non insulated Cemented carbide cutting tool. From the simulation analytical results; Titanium carbide cutting tool when air cooled maintained constant temperature of 30 $^{o}$C, but insulated cutting tool has been increased the temperature rapidly. The Solid works Simulation results showed that the tools when its base is convected had the maximum temperature 130 $^{o}$C and 115 $^{o}$C respectively.

**(Yash et al., 2013)[19]** created a finite element analysis simulation model in order to obtain solutions of the cutting forces, specific cutting energy and adequate temperatures occurred at different points through the chip/tool contact region and the coating/substrate boundary for a range of cutting tool materials and defined cutting conditions. Interfacial temperature in machining played a major role in tool wear and also resulted in modifications to the properties of the work piece and tool materials. A general movement towards dry machining, for environmental reasons, it was increasingly important to understand how machining temperature have

been affected by the process variables involved (cutting speed, feed rate, tool geometry, etc.) and by other factors such as tool wear.

**(Habib, 2013)[2]** investigated the role of cryogenic cooling on the formation of chip, cutting temperature and force and developed analytical model for cutting temperature and force in turning 42CrMo4 steel under cryogenic cooling condition. The matlab code has been used to determine the modeled value of cutting force and cutting temperature under cryogenic cooling condition. From an economic viewpoint, it was evident that having knowledge about the machining responses such as, cutting forces, cutting temperature and work piece surface integrity at different cutting conditions have been highly desirable as a means of realizing cost savings, increased productivity, and efficiency and for preventing any hazard occurring to the machine, cutting tool or the deterioration of the quality.

**(Augustine et al., 2013)[20]** proposed the estimation of the temperature and the heat flux at the chip-tool interface using the inverse heat conduction problem technique. The shear energy created in the primary zone, the friction energy produced at the rake face- chip contact zone and the heat balance between the moving chip and the stationary tool have been considered. The temperature distribution solved using finite difference method. The temperature and heat flux fields for various machining conditions along with their sensitivities and the situations of progressive flank and crater wear of the tool with continued machining have been considered. The mathematical models and simulation results have been satisfactory agreed with experimental temperature measurements reported in that literature.

**(Pius et al., 2013)[21]** studied the effect of temperature distribution on cutting tool life and wear using finite element methods. From the

experimental, analytical and simulation results; the carbide cutting tool when air cooled maintained constant temperature of 298 K, but when the cutting tool is insulated the temperature increased rapidly. The FEM analysis and ANSYS simulation showed that the cutting tool when its base is convected has the maximum temperatures of 404 K and 386 K respectively. The same results were obtained in both cases when the cutting tool base has been insulated.

**(Kohir et al., 2014)[22]** investigated the effect of length and inclination of the flank wear land on the cutting forces, effective stress and temperature distribution using finite element simulations. The results of the study showed that, the flank wear land inclination has higher influence on the thrust force compare to wear land length. The length and inclination of flank wear land effected the maximum temperature in tool.

**(Pervaiz et al., 2014)[23]** analyzed the temperature distribution at the cutting tool by using the conventional finite element machining simulations coupling with computational fluid dynamic (CFD) model. The conventional finite element machining simulations have been conducted using DEFORM 2D to predict the heat generation and tool tip temperature during the cutting action. Computational fluid dynamics (CFD) simulations have been performed using ANSYS® CFX. CFD model which incorporated air as a cooling media to simulate the dry cutting and temperature distribution at the tool surface was obtained. The coupled numerical method showed temperature distribution on the cutting tool.

**(Marcelo et al. , 2014)[24]** proposed the estimation of heat flux at the chip-tool interface using inverse techniques. Factors which influence the temperature distribution at the AISI M32C high speed steel tool rake face during machining of a ABNT 12L14 steel workpiece were also

investigated. The temperature distribution was predicted using finite volume elements. A transient 3D numerical code using irregular and no staggered mesh was developed to solve the nonlinear heat diffusion equation. The inverse problem was solved using the function specification method. Heat fluxes at the tool-workpiece interface were estimated using inverse problems techniques and experimental temperatures. Tests were performed to study the effect of cutting parameters on cutting edge temperature. The results were compared with those of the tool-work thermocouple technique and a fair agreement.

**(Rajamani et al, 2015)[25]** studied the performance of the coated carbide tool by varying the cutting speeds with constant feed and depth of cut. DEFORM 2D finite element software has been used. The fully coupled thermal-mechanical finite element analysis accurately simulated the formation of chip and predicted the cutting load and temperature distribution. The results from FE simulations showed that the friction has a strong influence on cutting forces, thrust forces, chip geometry and cutting temperature. It was observed that, the tool–workpeice interface temperature increased with an increase in cutting speed.

**(Kumar et al., 2016)[26]** developed the finite element model using ABAQUS/Explicit to analyses the temperature effects in turning. A WC tool coated with TiN considered as tool and AISI 4340 Steel considered to be the workpeice. Johnson- Cook formulation employed to model the workpeice and simulations were conducted to examine the temperature distribution, deformation and cutting forces. The results demonstrated the influence of machining factors in the process of heat generation and distribution during turning.

**(Kundrák et al., 2017)[27]** presented an example of heat modelling of hard turning. The layer thickness on the workpiece surface reached high temperature was determined. In that layer different modifications occurred due to heat. It was found that the thickness of the layer affected by heat depend primarily on the feed and only secondarily on other cutting parameters. The cooling gradient of the layer was determined, allowing conclusions to be drawn on the re-tempering of the heated layer. The computational fluid dynamics method and a commercial software has been used for the modelling and proved to be suitable for the simulation analysis of the hard turning process.

**(Wang et al., 2017)[28]** solved practical machining problems by using finite element method to achieve the required accuracy and the highly reliability. The simulation models based on the material properties of the self-prepared $Si_3N_4$ (Silicon Nitride) insert and HT250 were created. Using these models, the results of cutting force, cutting temperature and tool wear rate were obtained, and tool wear mode was predicted after cutting simulation. These approaches developed as the new method for testing new cutting-tool materials, shortening development cycle and reducing the cost.

**(Ojolo et al., 2017)[29]** employed finite element method (FEM) to model the temperature distribution of a mild steel with a carbide cutting tool insert in an orthogonal machining. The finite element model was simulated with MATLAB and validated with experimental data. The FEM showed that the maximum temperature occured at the tool tip and the temperature decreases with distance away from the tool tip. It also showed that the minimum temperature occurred at the extreme end of the tool insert.

**(Coskun Islam, 2018)[4]** presented a finite difference method based on numerical model simulating the temperature distribution in the chip, tool,

and finished workpiece surface layer as a function of material properties, cutting speed, feed rate and tool-workpiece engagement period. It has been shown that the sliding and sticking contact zones affected the heat partition between the chip and tool significantly. The shorter sticking zone leaded to the higher amount of heat transmitted into the tool, hence maximum and average rake face temperatures increase. Increased sticking zone length aided the removal of heat with the disposed chip in the simulated cases. Two and three-dimensional temperature prediction results have been found to be very close to each other because the metal cutting process approximated as a plain strain deformation. Feed rate had an inversely proportional effect on rise-time to steady-state, lower feed rates leaded to faster response because of reduced chip mass. Thermal diffusivity of the workpiece material had a direct effect on the time-dependent response. Lower thermal diffusivity (i.e. Titanium) resulted in longer rise-times compared to high thermally conductive materials (i.e. Aluminum) under the similar cutting conditions. Increased feed rate and cutting speed caused a reduction in the percentage of heat that flowed into the tool that conformed to the experimental observations in the literature.

**(Ferreira et al., 2018)[30]** presented an analysis of the thermal effects of coating in a carbide tool during a turning process using the COMSOL® software and a nonlinear inverse problem. The thermal model consisted of a coated carbide tool, a tool holder, and a shim represented by the transient three-dimensional heat diffusion equation with heat loss by convection and radiation. The heat flux, previously unknown, obtained through the function specification method. Titanium nitride (TiN) and aluminum oxide ($Al_2O_3$) have been utilized as the coating materials. Both coatings presented the expected behavior when less heat is dissipated to the cutting tool substrate. The coated carbide tools presented higher temperatures than the

uncoated carbide tool in the contact area. The study also found that the thicker the coating, the higher the temperature in the contact area. The results presented in this work helped the development of new long-lasting coated carbide tools.

**(Mohan Reddy et al., 2018)[31]** investigated the finite element modeling on machinability of Ti-6Al-4V using cubic boron nitride and polycrystalline diamond tool in dry turning environment. The analysis showed that depth of cut had the most influential parameter on resultant cutting force whereas feed rate had the most influential parameter on cutting temperature.

**(Akbar et al., 2018)[32]** focused the effect of cutting parameters (spindle speed, feed and depth of cut) on the response (temperature and tool life) during turning process. The inserts used in this study were carbide inserts coated with TiAlN (Titanium, Aluminum and Nitride) for machining a shaft of stainless steel 316L. Finite difference method has been used to find the temperature distribution. The experimental results were done using infrared camera while the simulation process performed using Matlab software package. The results showed that the maximum difference between the experimental and simulation results was equal to 19.3 °F, so, a good agreement between the experimental and simulation results was achieved. Tool life was decreased when spindle speed and feed were increased.

**(Kanellos et al., 2019)[33]** calculated the convective the thermo-mechanical part of the simulation, as well as a model in ANSYS CFX software for the simulation of the action of the heat transfer coefficient of a turning process, using a hybrid FEM-CFD model. The model consisted cutting fluid on the cutting tool. After validation of the model performed,

the hybrid model was simulated for various of the coupling between a model in Abaqus/Explicit software for the thermo-mechanical part of the simulation, as well as a model in ANSYS CFX software for the simulation of the action of the conditions, i.e. for various cutting speeds and speeds of cut, thus obtained valuable results regarding the applicability and cutting fluid on the cutting tool. After validation of the model was performed, the hybrid model was simulated for various efficiency of the proposed approach. Conditions, i.e. for various cutting speeds and speeds of cut, thus obtained valuable results regarding the applicability and efficiency of the proposed approach.

**(Tu et al., 2019)[34]** introduced finite element method (FEM) simulation to determine the temperature distribution of CBN/diamond coatings on silicon nitride ($Si_3N_4$ ) cutting tools with various parameters compared with titanium aluminum nitride (TiAlN) coatings. The results showed that the temperature increased with the increase of cutting speed while decreased with the increase of tool rake angle. The temperature of CBN-coated tools has been decreased by approximately 20.4–28.6% than TiAlN-coated tools under identical conditions.

**(Sahoo, 2019)[35]** deals with finite element analysis and prediction of physical parameters during hard turning of AISI4340 steel with ceramic tool insert by considering the effect of cutting parameters i.e. cutting speed , feed rate and depth of cut using DEFORM 3D. The methodology described expected to be highly beneficial to tool developers for complete understanding without performing costly and time consuming experiment.

**(Hussein et al., 2020)[36]** created a FEM simulation model in order to obtain numerical solutions for temperature distribution occurred at different regions through cemented carbide cutting tool insert. Temperature at tool-

chip interface has been determined by using empirical relation, it considered as boundary conditions in one side of insert. Finite element method was used as a numerical solution to calculate the temperature distribution at the given boundary conditions that specified. CUMSOL simulation showed the contour of temperature distribution in cutting tool insert.

**(J. Zhang et al., 2021)[37]** focused on the cutting temperature in transient heat conduction with a coated tool. A new analytical model to characterize the thermal shock based on the non-Fourier heat conduction was proposed. The distribution of cutting temperature in mono-layer coated tools during the machining was then illustrated. The cutting temperature distribution predicted by the Fourier heat conduction model was employed to compare with that by non-Fourier heat conduction in order to reveal the non-Fourier heat conduction effect in transient heat conduction. The results showed that the transient heat conduction analytical model was more suitable for the intensity transient-state and transient-state in the process of cutting heat conduction.

**(Guo et al., 2021)[38]** proposed a new heat source that caused the thermal error of the cutting tools. The potential energy of the tools' bending and twisting has calculated using experimental data, and how tool potential energy transformed into heat via friction is explored based on the energy conservation. The temperature rise of the cutting tool was simulated by a lattice-centered finite volume method. To verify the model, the temperature separation of a tool edge has been measured experimentally under the given cutting load. The results of the numerical analysis showed that the rise in tool temperature caused by the tool's potential energy was related to the time and position of the cutting edge involved in milling. For the same

conditions, the predicted results were consistent with the experimental results. The proportion of temperature rise due to tool potential energy was up to 6.57% of the total tool temperature rise. The results obtained the foundation for accurate thermal error modeling, and also provided a theoretical basis for the force–thermal coupling process.

**(Mohammed, 2022)[39]** investigated numerically by ANSYS fluent software the effects of heat transfer and heat flux on cutting tools with materials of $Al_2O_3$, $ZrB_2$, $TiB_2$, TiN. The influence of the machining parameters such as cutting speed and feed rate on the temperature and tool life has been investigated to indicate the optimum cutting tool and situation. The results showed that Zirconium diboride ($ZrB_2$) and Titanium diboride ($TiB_2$) had a temperature less than the aluminum oxide (Al2O3) so that the productivity would increase with the diboride materials utilized as cutting tool. Titanium diboride ($TiB_2$) materials achieved the maximum cutting tool life comparing to other materials.

## 2.2 Experimental Methods

**(Komanduri et al., 2001)[5]** developed several techniques for the measurement of heat and the temperatures generated in various manufacturing processes and tribological applications. They included: (1) thermocouples, (2) the embedded thermocouple and the dynamic infrared photography, (3) infrared optical pyrometers, (4) thermal paints, (5) materials of known melting temperatures, either in the powder form, or, as a thin film, and (6) change in microstructure with temperature in the case of high-speed steel tools, to name some. Each technique had its own advantages and disadvantages. The appropriated technique for a given thermal problem depend on the situation under consideration, such as the

ease of accessibility, spot size, dynamics of the situation, accuracy needed, cost of instrumentation, advancements in technology.

**(Outeiro et al., 2004)[40]** analyzed the temperature distribution in the three-dimensional cutting process experimentally. Specially designed thermal imaging equipment, included both hardware and software that developed in order to determine the temperature distribution in the deformation zone. A detailed description of this equipment, its calibration procedure and a full analysis of the emissivity of the cutting system components (chip, tool, and work piece) have been discussed. The designed thermal imaging equipment was proven to be very powerful to analyze the influence of the cutting parameters (cutting speed, cutting feed, depth of cut, work material, tool geometry, and tool material) on this temperature distribution. This equipment was useful for the construction and validation of numerical and analytical models of the three-dimensional cutting process.

**(Liljerehn et al., 2009)[41]** compared an analytical model for prediction of heat generation in the primary and secondary deformation zones with results from finite element simulations and temperature measurements using IR-CCD camera. The used cutting data have been altered to study the temperature influence from tool geometry and feed when machining stainless steel SANMAC316L and low carbon steel AISI 1045**.**

**(LB & M, 2010)[42]** measured the tool-chip interface temperature experimentally during turning of EN-31 steel alloy with tungsten carbide inserts using a tool-work thermocouple technique. First and second- order mathematical models have been developed in terms of machining parameters by using the response surface methodology on the basis of the experimental results. The metal cutting parameters considered were cutting

speed, feed rate, depth of cut and tool nose radius. It can be seen from the first order model that the cutting speed, feed rate and depth of cut were the most significantly influencing parameters for the chip-tool interface temperature followed by tool nose radius. Another quadratic model showed the variation of chip-tool interface with major interaction effect between cutting speed and depth of cut (V&D) and second order (quadratic) effect of cutting speed ($V_c$) appeared to be highly significant. The results showed that increase in cutting speed, feed rate and depth of cut increased the cutting temperature while increasing nose radius reduced the cutting temperature.

**(Haddag et al., 2013)[43]** dealt with a new modelling strategy, based on two steps of calculation, for analysis of the heat transfer into the cutting tool. Unlike the classical methods, considering only the cutting tool with application of an approximate heat flux at the cutting face, estimated from experimental data (e.g. measured cutting force, cutting power), the proposed approach consisted of two successive 3D Finite Element calculations and fully independent on the experimental measurements; only the definition of the behavior of the tool-workpiece couple was necessary. The first one was a 3D thermo mechanical modelling of the chip formation process, which allowed for estimating cutting forces, chip morphology and its flow direction. The second calculation is a 3D thermal modelling of the heat diffusion into the cutting tool, by using an adequate thermal loading (applied uniform or non-uniform heat flux). This loading has been using some quantities obtained from the first step calculation, such as contact pressure, sliding velocity distributions and contact area. Comparisons in one hand between experimental data and the first calculation and at the other hand between measured temperatures with embedded thermocouples

and the second calculation showed a good agreement in terms of cutting forces, chip morphology and cutting temperature.

**(Kulkarni et al., 2014)[44]** presented experimental results of dry, high speed turning of AISI 304 austenitic stainless steels using AlTiCrN coated cemented carbide insert. AlTiCrN coating was deposited on cemented carbide insert using 'cathodic arc evaporation (CAE)' PVD technique. Scanning electron microscope (SEM) was used to examine the coating morphology and coating thickness respectively. Micro-hardness, coating thickness and adhesive strength of coating was found to be 30 GPa, 3.8 μm and 89 N respectively. The turning tests were conducted at cutting speeds in the range of 140 to 320 m/min, feed in the range of 0.08 to 0.26 mm/rev keeping depth of cut constant at 1 mm. The influence of cutting parameters and tool coating were investigated on cutting force and cutting temperature. A tool-work thermocouple principle was used to measure the interface temperature during turning. The correlations between the cutting parameters cutting force and cutting temperature have been developed by minimizing the least squares error between experimental and predicted values of cutting force and cutting temperature. The correlation coefficient found close to 0.95. Cutting speed was found to be the dominant parameter for the cutting temperature whereas cutting force gets mostly affected by feed.

**(Kato et al., 2014)[45]** reported a new method to measure the temperature distribution in cutting tool. In this method, a thin PVD (physically vapor deposited) film deposited on a cutting tool was used as a thermal sensor. Various films of different materials were deposited to determine the location of a multiplicity of isotherms at different temperatures. Cemented carbide tools and alumina ceramic tools were used for tests. It has been

confirmed that the boundary between the melted film zone and the un melted film zone showed the isotherm directly and clearly. The method was also found to be very sensitive and applicable to any tool material as well as to a very small area.

**(Kus et al., 2015)[6]** estimated tool temperature by simultaneous temperature measurement employing both a K-type thermocouple and an infrared radiation (IR) pyrometer to measure the tool-chip interface temperature. The thermal analysis results were compared via the ANSYS finite element method. Experiments were carried out in dry machining using workpiece material of AISI 4140 alloy steel that was heat treated by an induction process to a hardness of 50 HRC. A PVD TiAlN-TiN-coated WNVG 080404-IC907 carbide insert was used during the turning process. The results showed that with increasing cutting speed, feed rate and depth of cut, the tool temperature increased; the cutting speed was found to be the most effective parameter in assessing the temperature rise. The heat distribution of the cutting tool, tool-chip interface and workpiece provided effective and useful data for the optimization of selected cutting parameters during orthogonal machining.

**(Mzad, 2021)[46]** used a spline cubic interpolation to estimate the transient heat flux imposed on the surface of a carbide cutting tool during stock removal, at constant thermal properties and cutting velocity. Interpolation of instantaneously measured temperature data set by the polynomial of lowest possible degree that passed through the points of the dataset was obtained. A high-precision remote-sensing infrared thermometer has been used to measure the temperature at the surface. For friction shear stress determination, a mounted sensing system detected strain gauges signals and computed them in the form of forces on the display screen. From thermal

behavior point of view the final result was notably interesting: it highlighted the feature of non-proportionality in temperature/heat flux variation.

## 2.3 Summary

| Year | Authors, Number of Reference | Objective of Study |
|---|---|---|
| 2015 | (D.Rajamani & A.Tamilarasan) | Studied the performance of the coated carbide tool by varying the cutting speeds with constant feed and depth of cut 1mm. DEFORM 2D finite element software has been used. |
| 2016 | (Kumar et al.,) | Developed the finite element model using ABAQUS/Explicit to analyses the temperature effects of turning. |
| 2017 | (Kundrák et al.,) | The computational fluid dynamics method and a commercial software was used for the modelling and proved to be suitable for the simulation analysis of the hard turning process. |
| 2017 | (Ojolo et al.,) | Employed (FEM) to model the temperature distribution of cutting tool insert in an orthogonal machining. The finite element model was simulated with MATLAB. |
| 2018 | (Ferreira et al.,) | Presented an analysis of the thermal effects of coating in a carbide tool during a turning process using the COMSOL software and a nonlinear inverse problem. |
| 2018 | (Mohan Reddy et al.,) | Investigated the finite element modeling on machinability of Ti-6Al-4V using cubic boron nitride and polycrystalline diamond tool in dry turning environment. |
| 2019 | (Tu et al.,) | Introduced (FEM) simulation to determine the temperature distribution of CBN/diamond coatings on silicon nitride (Si3N4) cutting tools with various parameters. |
| 2022 | (Mohammed et al.,) | investigated numerically by ANSYS fluent software the effects of heat transfer and heat flux on cutting tools. |

## 2.4 Motivation of this work

The machining manufacturing process has been extensively explored, with several experimental observations and numerical models generated. Much of this research is centered on understanding the machining process and designing tools that can reliably predict a variety of results. This knowledge might then be applied to the manufacturing industry, where manufacturing processes could be improved for reduced prices and superior performing products.

# CHAPTER THREE

# NUMERICAL ANALYSIS

# CHAPTER THREE

# Numerical Analysis

## 3.1Thermal Aspects of Metal Machining

Considerable heat is generated at the cutting edge of the tool due to friction between tool and work, and the plastic shearing of metal in the form of chips, when machining metal on a machine tool. The heat is evolved in three zones as shown in Figure 3.1.

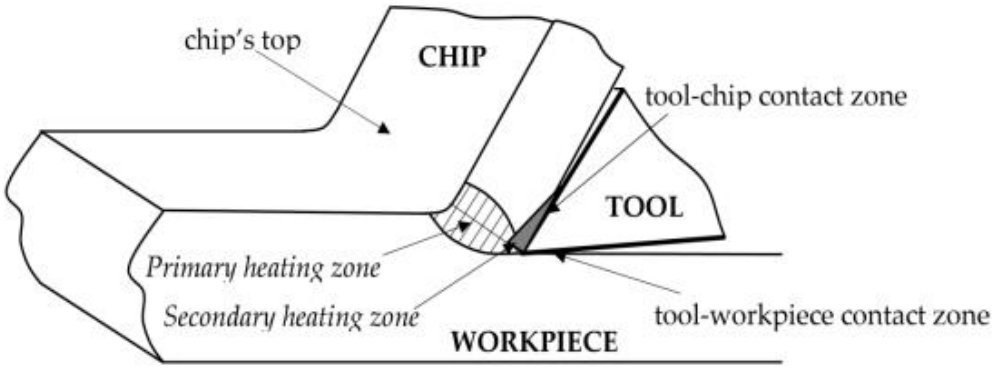


Figure 3.1 Evolution of heat at three zones **[8]**

In shear zone, maximum heat is generated because of the plastic deformation of metal, and practically all of this heat is carried away by the chip as machining is rapid and continuous process. Avery minor portion of this heat (5-10%) is conducted to work piece. In friction zone, the heat is generated mainly due to friction between moving chip and tool face and partly due to secondary deformation of the built up edge. In work-tool contact zone, the heat is generated due to burnishing friction and the heat in this zone goes on increasing with time as the wear land on the tool develops and goes on

increasing. It will be noted that each of these three zones leads to rise of temperature at the tool chip interface and it is found that the maximum temperature occurs slightly away from the cutting edge, and not at the cutting edge **[8].**

## 3.2. Heat generation

As a first approximation, it can be assumed that all of the mechanical energy associated with cutting or chip formation is converted into thermal energy. The energy that is not converted into thermal energy, such as the energy retained in the chips and that associated with the generation of the new surface area is negligibly small. It has been often assumed that the chip is formed instantaneously at the shear plane, so that a uniform plane source and velocity discontinuity may be assumed to exist there. The secondary deformation zone has usually been neglected and the tool–chip interfacial friction heat source taken as uniform. However the secondary shear zone is negligibly small at lower cutting speeds. The heat sources are estimated based on the measured shear stress and shear strain rate relations in the deformation zones as follows (Majumdar et al., 2005)**[10]:**

### 3.2.1. Primary zone

Assuming that the work of deformation is the energy converted into thermal energy, the rate of heat generation per unit deformed volume is expressed as **[10]**:

$$\dot{q} = \tau\dot{\gamma} = \sigma\dot{\varepsilon} \qquad (3\text{-}1)$$

Where:

$\tau$ : Shear stress

$\dot{\gamma}$ : Max. Shear strain rate

$\sigma$ : Unaxial stress

$\dot{\varepsilon}$ : Unaxial strain rate

The stress and the strain rate have to be estimated from the experimental data or relations.

### 3.2.2. Secondary zone

The plastic deformation in the secondary zone is strongly influenced by the cutting speed. At low cutting speeds, there is only frictional drag of the chip along the rake face. Under such cases, the secondary zone can be considered as a plane frictional heat source with minor error. This frictional heat generation rate per unit area at a point on the contact length is estimated as **[10]:**

$$\dot{q}_x = \tau_x V_x \quad (3\text{-}2)$$

At higher cutting speeds, the secondary zone heat source is more spread out. Observation of deformed grids indicated that a triangular region might approximate the secondary zone. For normal cutting condition there is a plastic state of stress in the chip adjacent to the tool–chip interface along most of the contact length. Only towards the end of the contact, where the chip starts to curl away from the tool, the stress becomes elastic. Assuming that the elastic part of the contact is negligible and assuming that the interface is in the direction of maximum shear stress, the shear flow stress is estimated as,

$$\tau_{sec} = \frac{F_f}{H_{w1}} \quad (3\text{-}3)$$

Where $F_f$ the friction force along the interface, H is the contact length and $w_1$ is the width of cut.

Also, assuming that the interface is in the direction of maximum shear strain rate and the velocity changes from zero at the tool face to bulk chip velocity $V_c$ across the plastic zone thickness $t_p$, the maximum strain rate is estimated as:

$$\dot{\gamma}_{sec} = \frac{V}{t_p} \tag{3-4}$$

The maximum thickness of the plastic zone is expressed as

$$t_p = \delta t^2 \tag{3-5}$$

The heat generation rate per unit volume at any point in the secondary zone is expressed as

$$\dot{q}_s = \tau_{sec}\dot{\gamma}_{sec} \tag{3-6}$$

Eqs. (3-2)– (3-6) are used to establish heat generation in the secondary zone.

## 3.3 Friction Model

Coulomb's friction model is used to describe the tool/chip interface friction. Following this, we can see there are two regions on the rake face of the cutting tool: the sliding region and the sticking region, as shown by Figure 3.2. The sliding region is defined by a constant coefficient of friction, μ. The sliding region interface frictional stress, $\tau_{fr}$ can be expressed as

$$\tau_{fr} = \mu\sigma_n \quad \text{if} \quad \tau_{fr} < \bar{\tau}_{max} \tag{3-7}$$

Where $\sigma n$ is the normal stress. Conversely, the sticking region is defined by an equivalent shear stress limit, $\bar{\tau}_{max}$. The sticking region interface frictional stress can therefore be expressed as:

$$\tau_{fr} = \bar{\tau}_{max} \quad \text{if} \quad \tau_{fr} \geq \bar{\tau}_{max} \tag{3-8}$$

Where $\bar{\tau}_{max} = \frac{\bar{\sigma}_s}{\sqrt{3}}$ and $\bar{\sigma s}$ is the Von-Mises equivalent stress **[47].**

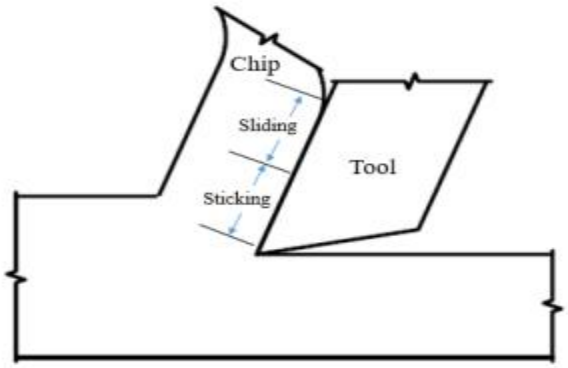


Figure 3.2: Sticking and sliding friction regions between tool and chip interface **[47].**

## 3.4 Heat Transfer Model

During machining, heat generation occurs due to high plastic deformations taking place in the shear zone, as well as the friction heat produced at the tool-chip interface. The heat generated due to plastic strain is expressed as **[48]:**

$$\dot{q}_p = \eta_p \, \sigma_{eqv} . \dot{\varepsilon}^{pl} \quad (3\text{-}9)$$

Where $\dot{q}_p$ is volumetric heat flux due to plastic work, $\eta_p$ is the fraction coefficient of energy converted to heat for plastic work, $\sigma_{eqv}$ is the equivalent stress, $\dot{\varepsilon}^{pl}$ is the plastic strain rate. Heat generation due to friction at the tool-chip interface can be expressed as

$$\dot{q}_f = \eta_f \tau_{fr} V_s \quad (3\text{-}10)$$

Where $\dot{q}_f$ is the volumetric heat flux due to frictional work, $\eta_f$ is the fraction coefficient of energy converted to heat for frictional work, $V_s$ is the sliding velocity

Heat balance equations at the tool–workpiece interface are written,

$$\bar{\bar{q}}_{\rightarrow tool} = \beta \dot{q}_f + \dot{q}_c \quad (3\text{-}11)$$

$$\bar{\bar{q}}_{\rightarrow workpeice} = (1-\beta)\dot{q}_f - \dot{q}_c \quad (3\text{-}12)$$

Where

$$\bar{\bar{q}}_c = h(T_w - T_t) \quad (3\text{-}13)$$

The introduction of Eqs. (3-10) and (3-13) in (3-11) & (3-12) leads to the following heat balance equations of the tool–workpiece interface:

$$\bar{\bar{q}}_{\rightarrow tool} = \beta\eta_f\tau_{fr}V_s + h(T_w - T_t) \quad (3\text{-}14)$$

$$\bar{\bar{q}}_{\rightarrow workpeice} = (1-\beta)\eta_f\tau_{fr}V_s - h(T_w - T_t) \quad (3\text{-}15)$$

where $\bar{\bar{q}}_{\rightarrow tool}$ and $\bar{\bar{q}}_{\rightarrow workpeice}$ are heat flux densities going into the tool and workpiece, respectively, $\beta$ is the heat generation coefficient which defines the fraction of friction heat generated in the tool side ($\beta\dot{q}_f$) and the complementary part $[(1-\beta)]\,\dot{q}_f$ in the work material side, h is the heat transfer coefficient, $\bar{\bar{q}}_c$ is the heat conduction flux, and $T_w$ and $T_t$ are temperatures, respectively, on two elemental surfaces in the workpiece and tool under contact.

## 3.5 Methodology to perform Explicit Dynamics Simulations

Finite element models are created in Explicit dynamic. In order to simulate 3D orthogonal machining processes, a powerful general purpose finite element analysis package. Ansys is a finite element analysis package to numerically solve a wide variety of mechanical, structural and non-structural problems. These problems include static/dynamic structural analysis (both linear and non-linear), heat transfer and fluid problems as well as acoustic and electromagnetic problems. A model was developed for simulation of temperature distribution in tool-chip interface based on the contact stresses estimated earlier. The models are run as a coupled thermal-mechanical analyses in order to include thermal effects. As cutting occurs, it generates a large amount of heat which cause

thermal effects that in turn, largely impact mechanical behavior. There are two basic approaches for studying machining processes 1. Minimum energy principle and 2. Slip-line field theory. In the minimum energy principle, it is assumed that the plastic deformation occurs only in the shear plane. So the cutting energy is calculated from the shear strain and the shear stress at the shear plane. In the slip-line field theory, it is assumed that the continuous chip formation in the shear zones, i.e. continuous plastic deformation around the shear plane. The present study is based on the Minimum energy principle theory. The analysis procedure consists of three phases such as pre-processing, solution and post processing. The Pre-processing phase consists of defining geometry, material, mesh and boundary conditions. The solution phase consists of defining analysis settings and convergence. The post processing phase consists of obtaining results.

## 3.6 DESIGN AND MODELLING

The geometry of machining process was created by using the Solid-work software. A number of objects are created to get the final shape of the geometry with the following procedures:

The geometry device shown in Figure (3.3) consists of a workpeice with a length, height and width of (150 mm) (50 mm) (30mm) respectively. The tool made with rake angle of $6^0$. Here cutting tool and workpeice considered as flexible body.

The analysis has been performed for different depth of cuts and by altering the cutting speed while maintaining a constant feed rates. It can be inferred that

three different depth of cuts (1.5 mm, 2 mm and 2.5 mm) have been employed. For these depth of cuts, the cutting speed was (6 m/s, 8m/s and 10 m/s).


Figure (3-3) Model Shape.

Meshing is made for the tool and work piece by assigning element size or by default meshing size. The meshed body and boundary conditions, show in figure (3-4) and figure (3-5).

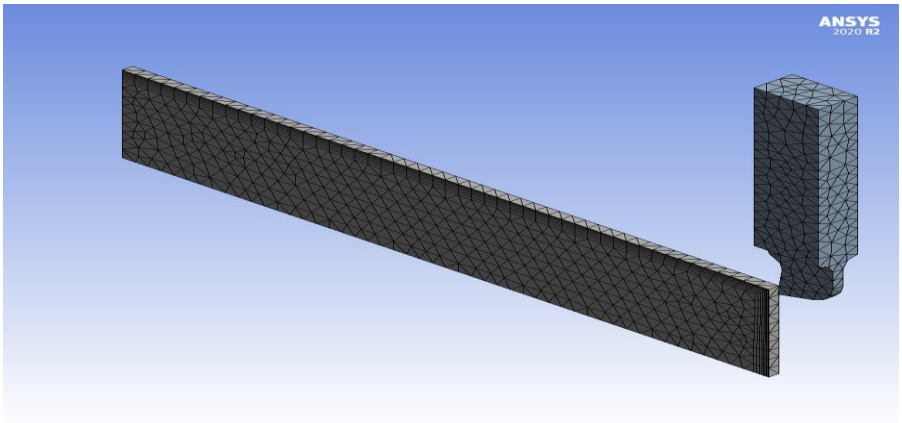


Figure (3-4) Model Mesh.

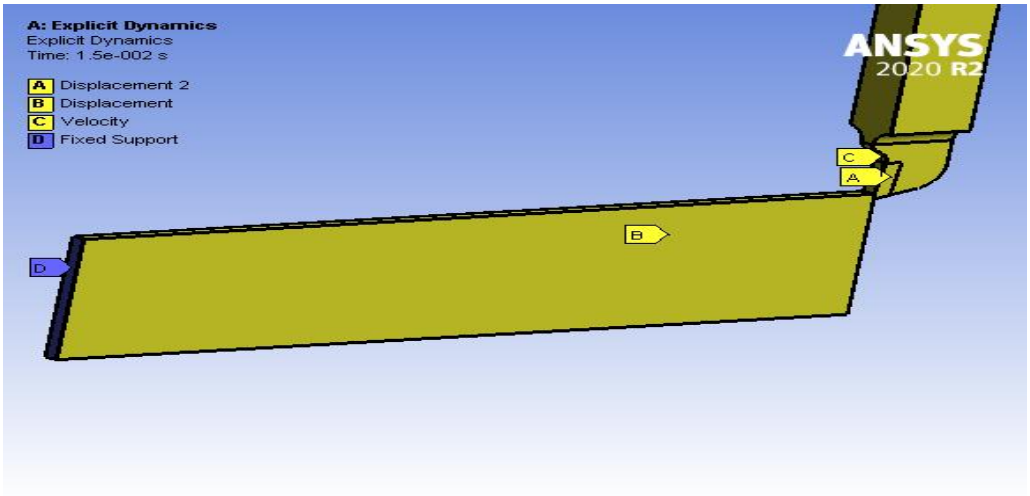


Figure (3-5) Model boundary conditions.

## 3.7 Methodology to perform CFD Simulations

Due to the fast improvement of computer science, the usage of computational fluid dynamics CFD has increased significantly in recent years. The basic numerical methods have been developed widely and applied in many research area and industries. The simulation packages become more complex and accurate. . However, as a consequence to this improvement in CFD science by using computerized programs, it is essential matter to solve any problems by using developed codes of numerical analysis in computer. This section contains the numerical analysis of the temperature distribution in cutting tool insert. The programming and graphical tools of the numerical analysis techniques are used to get mathematical models for many applications of civil ,chemical ,electrical and mechanical engineering take in approximating a complex for continuous surface of structure or process such as fluid flow mechanics, solid mechanics, stress analysis, torsion analysis, phenomena including heat transfer,

electricity, magnetism, quantum mechanics, relativistic mechanics and other engineering application as shown in **Numerical analysis**.

ANSYS 2020R2 used advanced numerical analysis with different procedures to find accurate results when suitable models are used.

### 3.7.1 Assumptions

The following assumptions are used to simplify the proposed model solution:

- Steady state conditions.
- Three dimensional.
- Radiation effects are negligible.
- The materials is solid and has constant properties.
- No slip at wall.
- The tool has constant cutting velocity.
- The depth of cut is constant.

### 3.7.2 Governing Equations

The governing equations to be solved are the continuity momentum and the equation of the energy **[49]:**

### A. Mass Conservation (Continuity)

$$\nabla.\left(\rho\vec{V}\right)=0 \tag{3-16}$$

Velocity vector components can be defined as following:

$$\vec{V}=\vec{u}i+\vec{v}j+\vec{w}k \tag{3-17}$$

For incompressible flow, substituting Eqn. (3-17) in (3-16) yield

$$\partial u \vec{} / \partial x + \partial v \vec{} / \partial y + \partial w \vec{} / \partial z = 0 \quad (3\text{-}18)$$

### B. Momentum Equation

The momentum equation is also known as Navier-The Stokes equation. And it has several different formulas and can be written as follows

$$u\frac{\partial u}{\partial x} + v\frac{\partial u}{\partial y} + w\frac{\partial u}{\partial z} = \frac{1}{\rho}\frac{\partial p}{\partial x} + v\left(\frac{\partial^2 u}{\partial x^2} + \frac{\partial^2 u}{\partial y^2} + \frac{\partial^2 u}{\partial z^2}\right) \quad (3\text{-}19)$$

$$u\frac{\partial v}{\partial x} + v\frac{\partial v}{\partial y} + w\frac{\partial v}{\partial z} = \frac{1}{\rho}\frac{\partial p}{\partial y} + v\left(\frac{\partial^2 v}{\partial x^2} + \frac{\partial^2 v}{\partial y^2} + \frac{\partial^2 v}{\partial z^2}\right) \quad (3\text{-}20)$$

$$u\frac{\partial w}{\partial x} + v\frac{\partial w}{\partial y} + w\frac{\partial w}{\partial z} = \frac{1}{\rho}\frac{\partial p}{\partial z} + v\left(\frac{\partial^2 w}{\partial x^2} + \frac{\partial^2 w}{\partial y^2} + \frac{\partial^2 w}{\partial z^2}\right) \quad (3\text{-}21)$$

### C. Energy equation

Since the density is constant for incompressible flows, the energy equation can be written as follows

$$\frac{\partial}{\partial t}(\rho H) + \nabla.(\rho \vec{v} H) = \nabla.(k\nabla T) + S \quad (3\text{-}22)$$

Where:

H: Enthalpy

$\rho$ : Density

$\vec{v}$ : Fluid velocity

S: Source term

## 3.8 Finite Volume Method (FVM) analysis of tool temperature

A 3-D model is develop for simulation of temperature distribution in cutting tools based on the contact temperature on tool-chip interface estimated earlier. The model based on the FVM. In the FVM software (ANSYS FLUNT) utilized

for the simulations, the temperature distribution is obtained from the balance of the heat generated and removed at steady state, and from the heat transport within the different parts of the system. The 3-D section at which the temperature distribution is calculated includes different material of tools (High speed steel, Ceramic, Carbide) the tool holder made of High speed steel.

## 3.9 The Boundary Conditions of CFD model

The thermal boundary conditions used were:

1. Heat convection to the surrounding air at all free($q^o = -k\frac{\partial T}{\partial n} = h_{air}(T - T_o)$).

2. Heat conduction through the front of the chip and through the lower boundary of the workpiece with material flow away from the tool.

3. Constant temperature ($T_o$ = 25°C) at the base of the tool support and at the upper boundary of the workpiece.

## 3.10 Thermal properties

Table (3.1) and (3.2) displays the properties of the materials used in manufacturing both tool and workpeice. The properties of (Aluminum, Iron, Copper, $Al_2O_3$ ceramic) are provided by the ANSYS materials library, while the properties of the (High speed steel) was taken from **(Kadhim et al., 2021)[50]** and carbide was taken from reference **(Miller, 2020)[51].**

Table (3-1) Thermal properties of tools

| Parameter | High Speed Steel | Carbide | $Al_2O_3$ Ceramic |
|---|---|---|---|
| Density($kg/m^3$) | 8138 | 11900 | 4500 |
| Thermal conductivity (W/m.°C) | 41.5 | 50 | 29 |
| Specific heat($J/Kg.^0C$) | 460 | 400 | 800 |

Table (3-2) Thermal properties of workpeices

| Parameter | Aluminum | Iron | Copper |
|---|---|---|---|
| Density($kg/m^3$) | 2710 | 7860 | 8933 |
| Thermal conductivity (W/m.°C) | 237.5 | 80 | 400 |
| Specific heat($J/Kg.^0C$) | 951 | 434 | 385 |

## 3.11 The Structure of CFD

The CFD code consists of the following three main features:

1. Pre-processor

2. Solver

3. Post-processor

**1. Pre-processor**

The pre-processor task is together the essential information needed for the solver to tackle the problem, i.e., the input. This involves:

- Defining the geometry of interest, i.e., the computational domain.
- Generation of the grid.
- Specifications of the physical and chemical phenomena that need to be modeled.
- Definition of the solid properties.
- Specification of appropriate boundary conditions.

**2. Solver**

The aim of the solver is to carry out the numerical calculations necessary to produce satisfactory simulations of the flow problem. The solver can base on some techniques such as, finite volume and finite element.The main differences between these techniques are based on how the variables of flow are approximated and on the discretization process.

Fluent uses a technique called the finite volume method (FVM). The numerical algorithm consists of the following structure:

- Integration of the governing equations of geometry over all the control volumes within the solution domain.
- Discretization involving substitution of a variety of finite difference-type approximations for the terms in the integrated equation representing the Cutting processes. The terms in question are convection, diffusion and

source terms. By doing this the system of integral Equations are transformed into a system of algebraic equations that can be solved numerically.

- Solution of the algebraic equations by an iterative method.

**3. Post-processor**

The post-processor returns the results of the simulation calculated by the solver. Today, most of the available CFD programs have been developed graphical tools, which make it possible to receive a visualization of the calculated data.

## 3.12 Simulation Setting

To setup the simulation in ANSYS Fluent, the following step should be carried out:

- The meshed geometry of simulation case study was imported into Fluent.
- The solids was defined.
- Specify the operation conditions.
- Defining the boundary condition concerned.
- Appropriate residual conditions were defined.
- Define number of iterations.

## 3.13 Geometry and Mesh Generation

### 3.13.1 Modelling Of Tool

The cutting tool has been solid modelled by using SOLIDWORKS, a solid modelling computer aided design software. Solidworks is a solid modeler, and utilizes parametric feature-based approach to create models and assemblies. Parameters refer to constraints whose values determine the shape of or geometry of the model or assembly. Parameters can be either numeric parameter, such as tangent, parallel, concentric, horizontal or vertical etc. numeric parameters can be associated with each other through the use of relations.

#### 3.13.1.1 Modelling Of HSS Tool

The cutting tool (HSS) has been solid modelled by using SOLIDWORKS. The 3D view is shown in below (Figure 3.6).

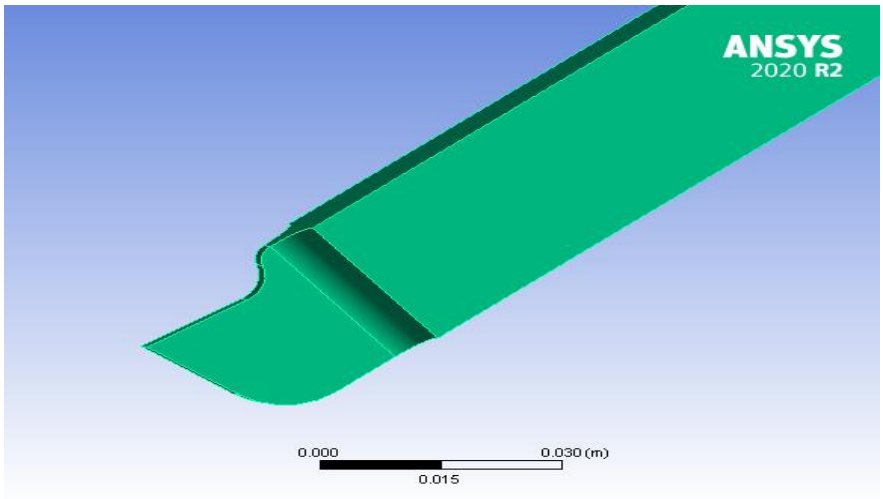


Figure (3-6) 3D view of HSS model

### 3.13.1.2 Modelling Of Carbide Tool

The cutting tool (Carbide) has been solid modelled by using SOLIDWORKS. The 3D view is shown in below (Figure 3.7).

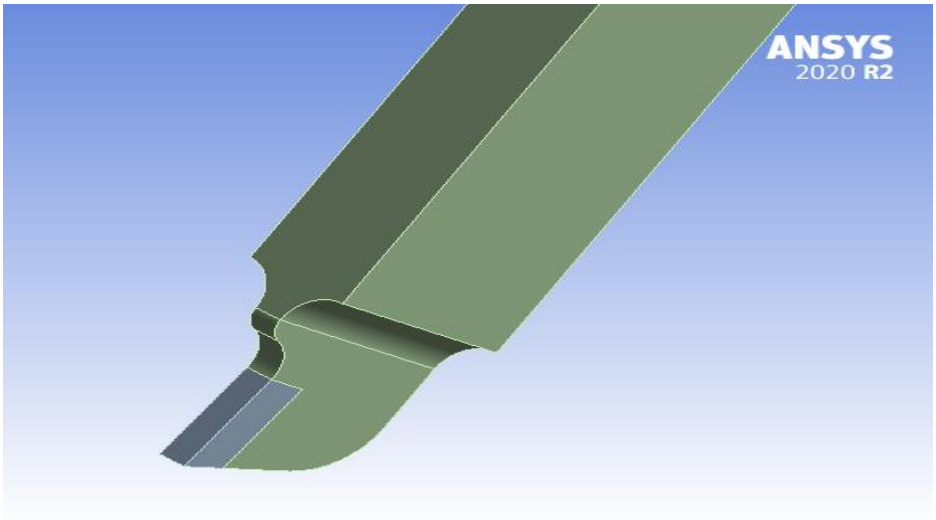


Figure (3-7) 3D view of Carbide model

### 3.13.2 The meshes

Normal CFD technique need a mesh which arrange the boundaries of the computational domain. The building of the computational mesh is appropriate to the discretized solution for the three dimensional continuity, momentum and energy equations. A good mesh is the last point of the total number for the cells generation, it is basis to have sufficient number of cells for a good determination but memory desires growth to the increasing for the number of cells, thus, the triangular elements is chosen with the free mesh in the present work as shown in fig. (3-8)& fig. (3-9). For the HSS tool the solid (wall) domains were meshed with [1316478] elements and (248987) nodes. Whereas for the carbide tool (carbide part is meshed with [2965] elements and [1264] nodes and the tool handle is meshed with [163297] elements and (31999] nodes.

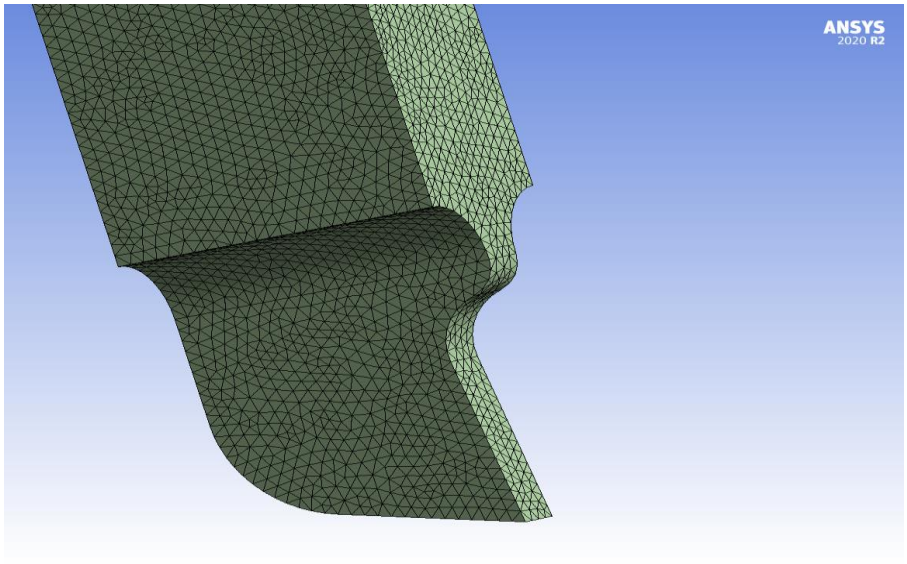


Figure (3-8) Meshed geometry of HSS tool

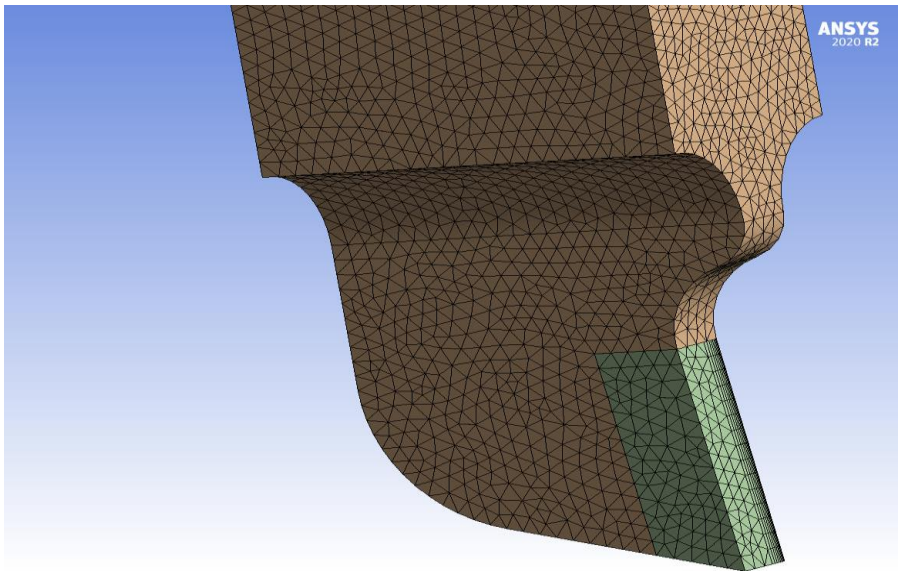


Figure (3-9) Meshed geometry of Carbide tool

## 3.14 Number of Iterations

The CFD technique requires iterating the solution of the fluid flow equations till it is converged. The convergence criteria selected when the results stay the same within the same accuracy. Error residuals are the commonly used method of verifying the convergence of the solution is the discrepancy between the values of a component in two successive iterations, multiplied for the first five iterations by the highest absolute residual. When the residuals are under a specified tolerance limit, the solution called converged. Figure (3.10) presents the simulation conversion process.

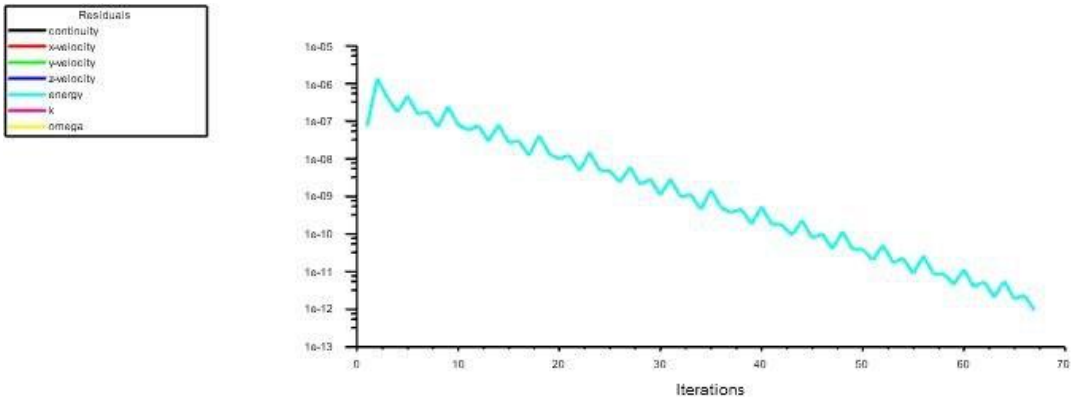


Figure (3.10): Results conversion.

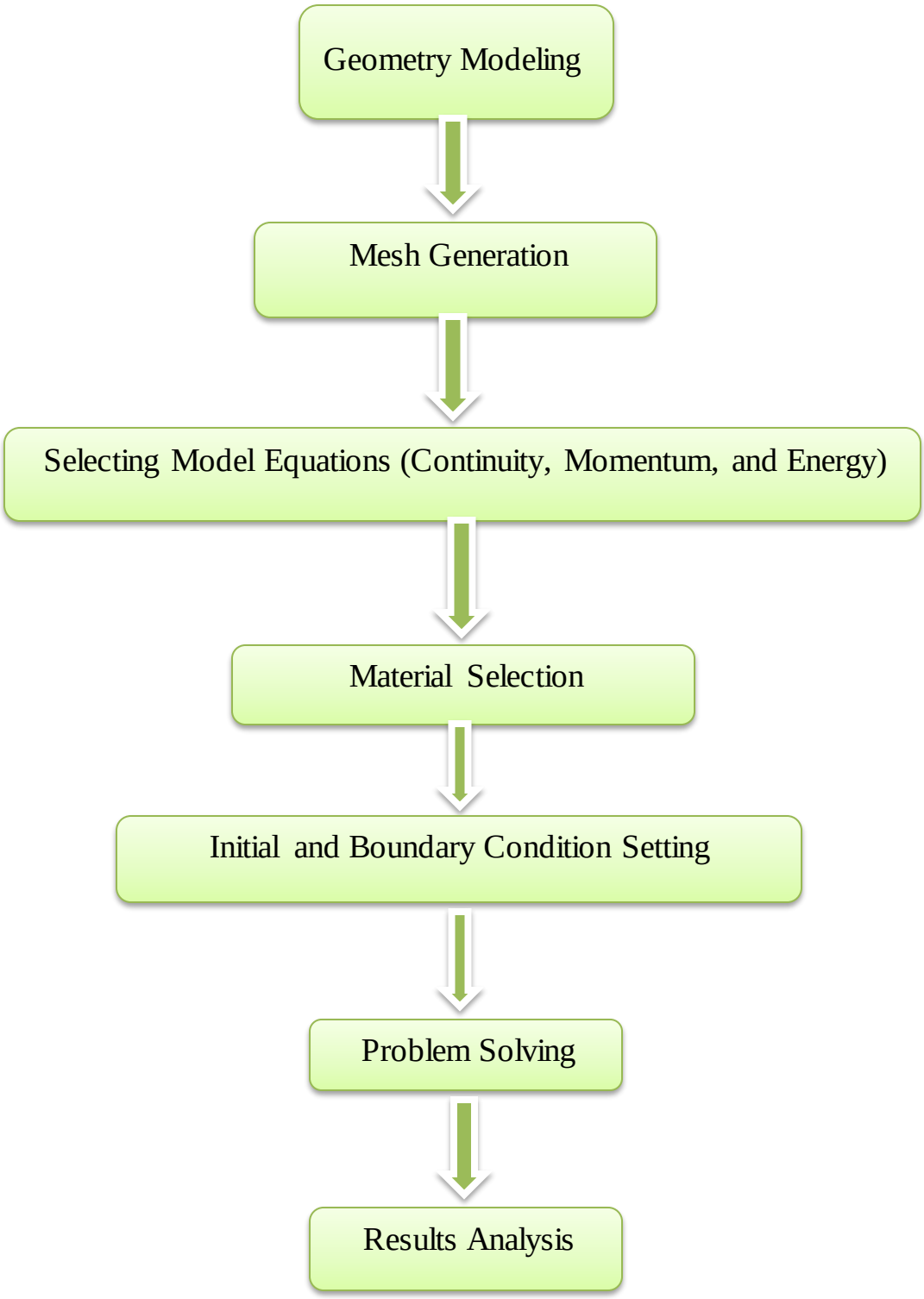


Figure (3-11): Numerical Simulation Chart

# CHAPTER FOUR

# RESULTS AND DISCUSSION

# CHAPTER FOUR

# RESULTS AND DISCUSSION

## 4.1 Introduction

Numerical results proposed cutting process temperature analysis approach is discussed here. Numerical analysis of the system is performed using ANSYS 2020 R2 to predict the temperature distribution in cutting process. For ease of discussion the results are divided into four parts which are:

1. Effect of changing the cutting speed on temperature distribution in cutting process.

2. Effect of changing the depth of cut on temperature distribution in cutting process.

3. Effect of changing type of tool material on cutting tool temperature.

4. Effect of changing type of work piece material on cutting temperature.

## 4.2 Validation

For validation of the simulation results, the temperature of the insert as an average value was compared with the same studies as shown in figure (4.1). It is indicated that the deviation between the results is very limited. Therefore, the validation results explained that the differences between the numerical and the experimental results are acceptable where the regular differences between numerical and previous results for average temperature is around 5. 25%. In general, the differences are acceptable for simulation errors. The temperature begins to increase when the heat flux was applied and it begins to decrease when

the cutting tool goes away from the workpiece and there is no heat flux. The tool interface temperature distribution applying to the conditions of **[Mohammed et al.,]** is illustrated in figure (4.2) at (10, 30, 60 and 80) seconds.

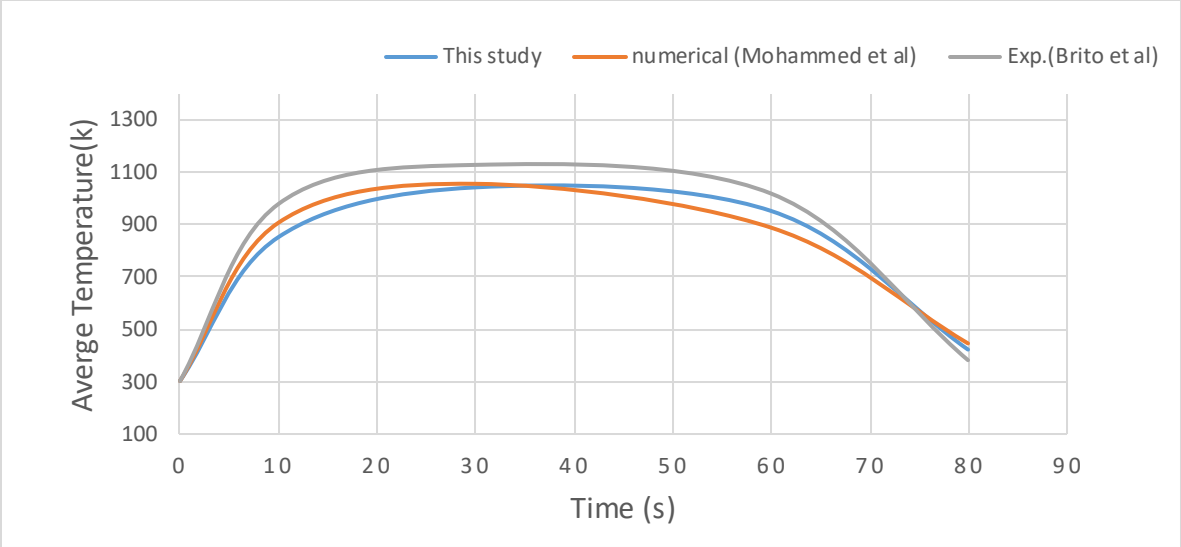


Figure (4.1) Comparison between the numerical results and the previous studies of **Mohammed et al. [39]** and **Brito et al.[51]** for the average temperature of the contact area during the cutting of $Al_2O_3$.

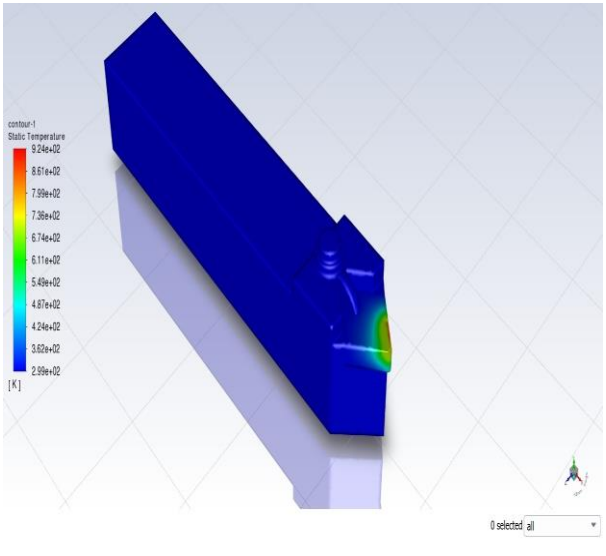

**(a)**

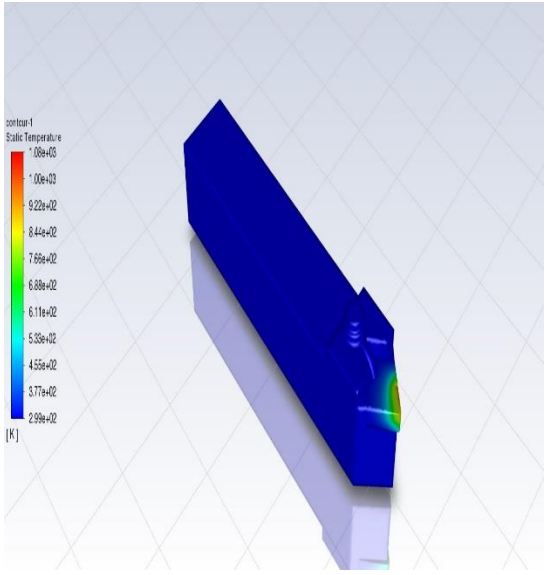

**(b)**

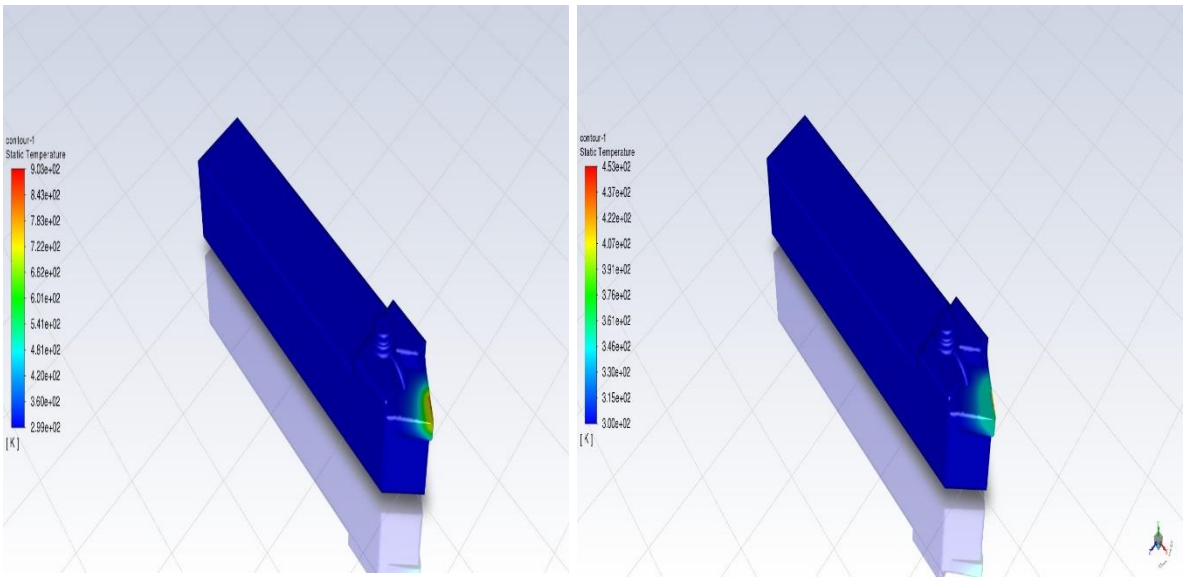


**(c)** **(d)**

Figure (4.2):Validation of the developed model against (Mohammed, 2022) at (a) 10 s (b) 30 s (c) 60 s (d) 80 s

## 4.3 Numerical Results

The ANSYS 2020 R2 program was utilize for modeling and simulation the cutting process in the present study. Sub programs have been used to complete the simulation of metal cutting. First one is Explicit dynamic, in this sub program simulate the movement of cutting tool with the depth of cut and the velocity of cutting process. The FEM technique were used to establish the simulation of cutting process. The temperature generated in the cutting process are a result parameter which in term used to complete the temperature distribution in both workpiece and cutting tool by using the second sub program, Fluent. ANSYS Fluent which utilized the FVM technique to solve the

continuity, momentum and energy equation of the incompressible three dimensional steady state.

The Minitab 17 program used to reduce the number of cases. The analysis was done for 27 different cases.

### 4.3.1 Temperature of Cutting Process

The temperature of cutting can be estimated by Ansys/Explicit dynamic. Due to high and constant temperature of chip also it continues contact with cutting tool surface it can be consider a constant temperature body (constant heat flux) that effects on the cutting tool insert. To study the effect of different process parameters on the cutting temperature values, each temperature value represents the average of cutting temperature during machining operation. It depends on the cutting speed, depth of cuts, material type of tool and workpeice. The temperature profile of cutting can be achieved by knowing the stress value between the workpiece and the cutting tool. Figure (4.3) shows the contour of Equivalent (Von-Mises) Stress of High Speed Steel cutting tool and Aluminum workpeice at depth of cut(1.5 mm) and cutting velocity varying from (6 m/s), (8 m/s) and (10 m/s). Figure (4.4) shows the contour of Equivalent (Von-Mises) Stress of Carbide cutting tool and Iron workpeice at depth of cut(1.5 mm) and cutting velocity varying from (6 m/s), (8 m/s) and (10 m/s). Figure (4.5) shows the contour of Equivalent (Von-Mises) Stress of Ceramic cutting tool and Aluminum workpeice at depth of cut(1.5 mm) and cutting velocity varying from (6 m/s), (8 m/s) and (10 m/s).

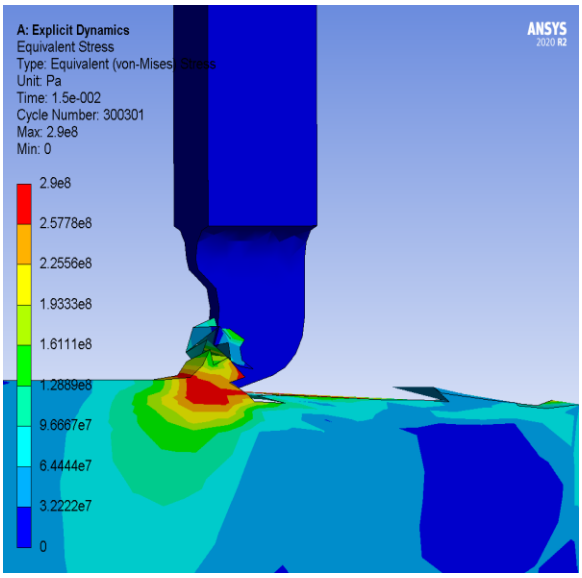


(a)

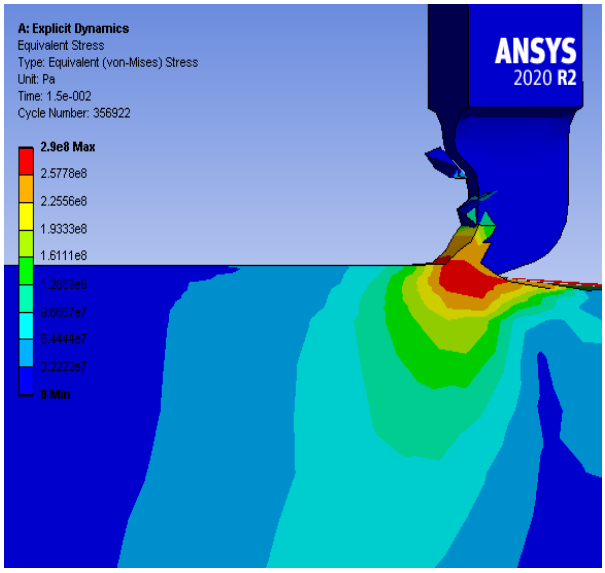


(b)

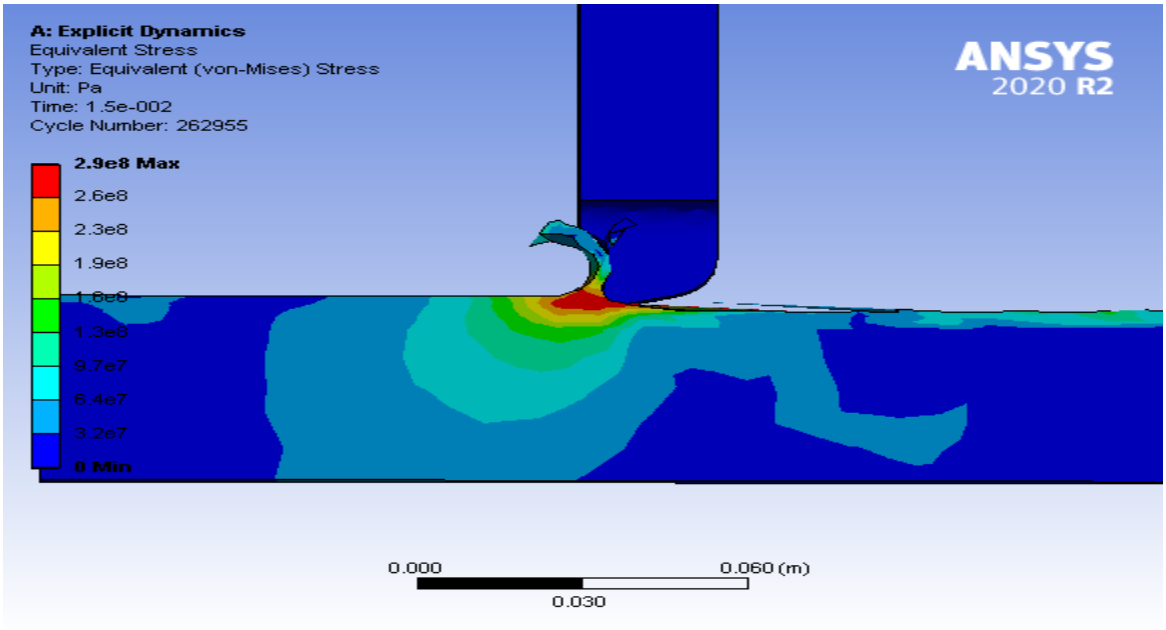


(c)

Figure (4.3) show contours of Equivalent (Von-Mises) Stress distributions of HSS cutting tool and Aluminum workpeice at DOC= 1.5 mm and (a) Vc= 6 m/s (b) Vc= 8 m/s (c) Vc= 10 m/s

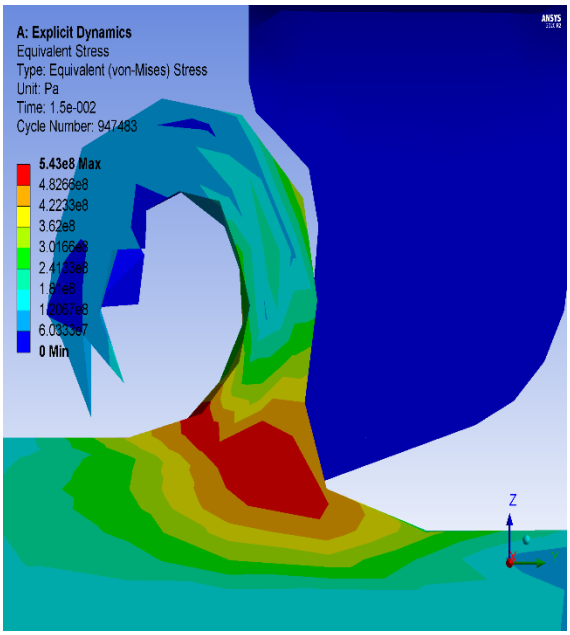


(a)

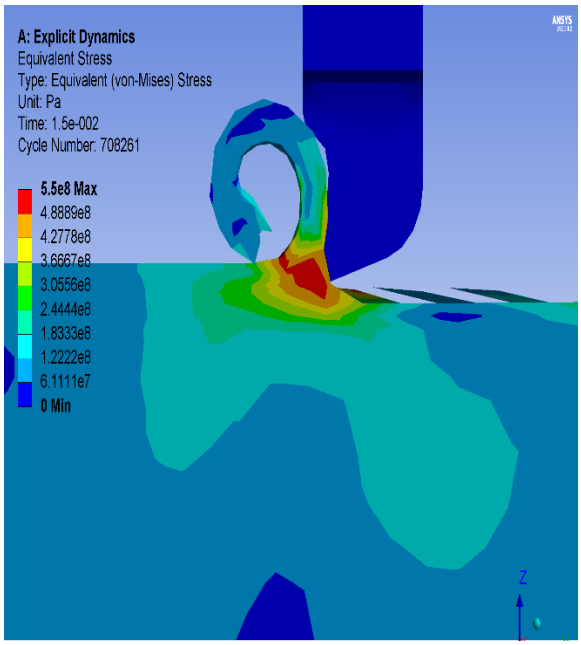


(b)

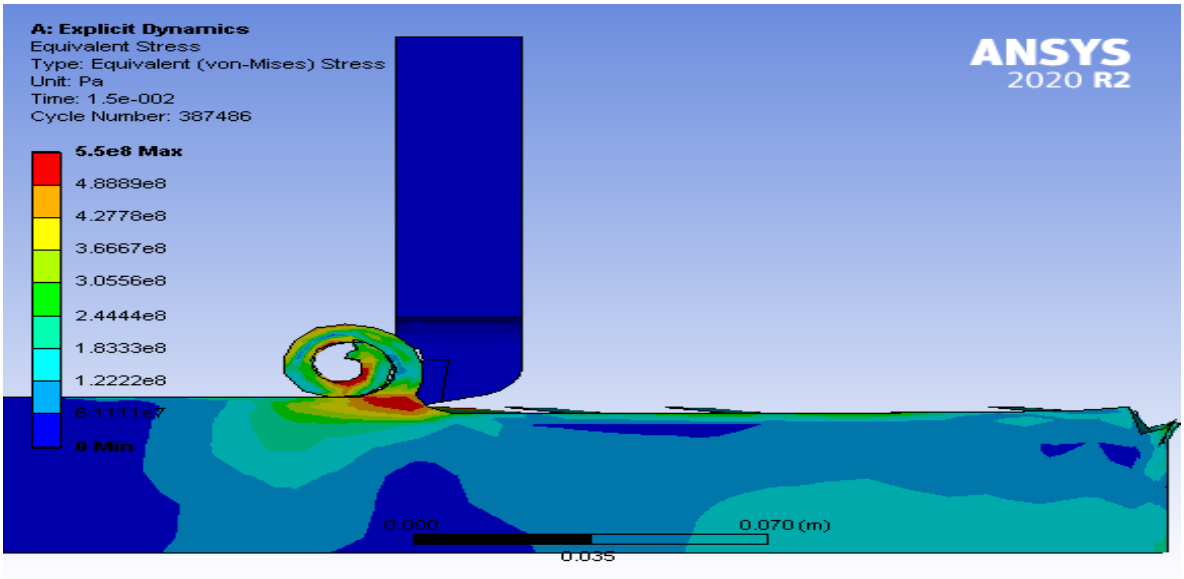


(c)

Figure (4.4) show contour of Equivalent (Von-Mises) Stress distributions of Carbide cutting tool and Iron workpeice at cutting depth= 1.5 mm and (a) Vc= 6 m/s (b) Vc= 8 m/s (c) Vc= 10 m/s

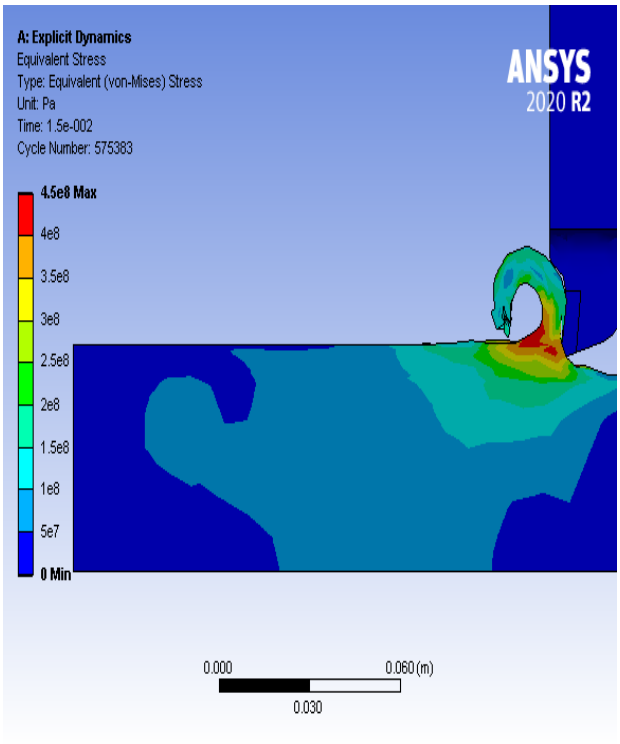


(a)

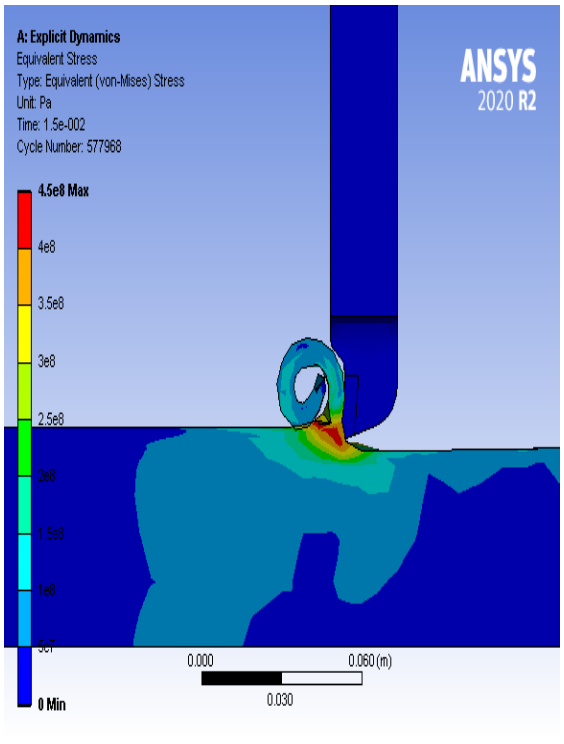


(b)

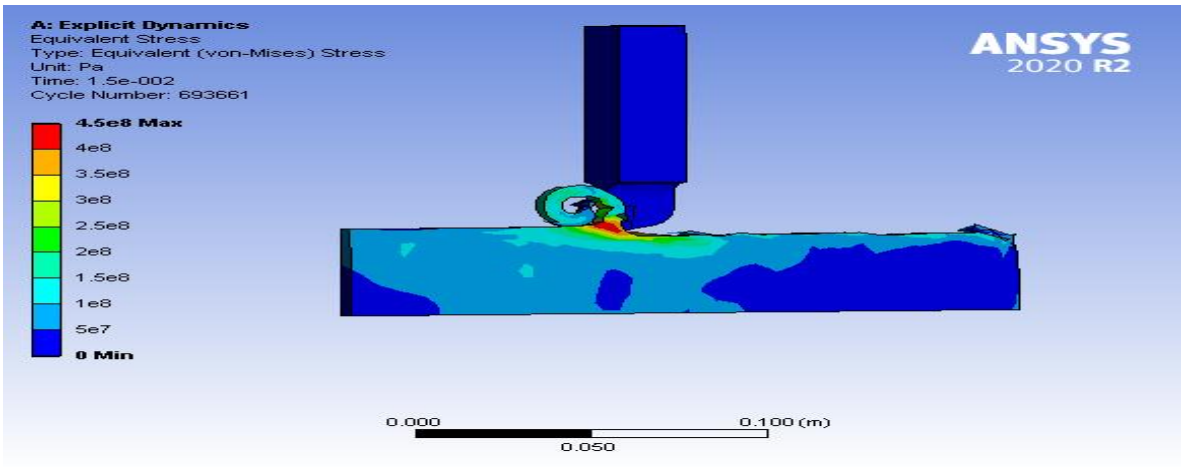


(c)

Figure (4.5) Show contours of Equivalent (Von-Mises) Stress distributions of Ceramic cutting tool and Copper workpeice at cutting depth= 1.5 mm and (a)Vc= 6 m/s (b) Vc= 8 m/s (c) Vc= 10 m/s.

From the figures above it can be shown that the distribution of Equivalent (Von-Mises) stress in the cutting deformation zone is similar to that of the three different cutting speeds, but the cutting speed has a greater influence on the cutting deformation. When cutting speed is increased, the Equivalent stress is mainly concentrated in the chip deformation, this leads to an increase in stresses in this region and thus an increase in temperatures. Figure (4.6), (4.7) and Figure (4.8) show the relation between the stresses and temperatures of (Aluminum, Iron & Copper) metal cutting, respectively at cutting speed (6, 8 & 10) m/s. They show that the temperature is increased with increasing the value of stresses.

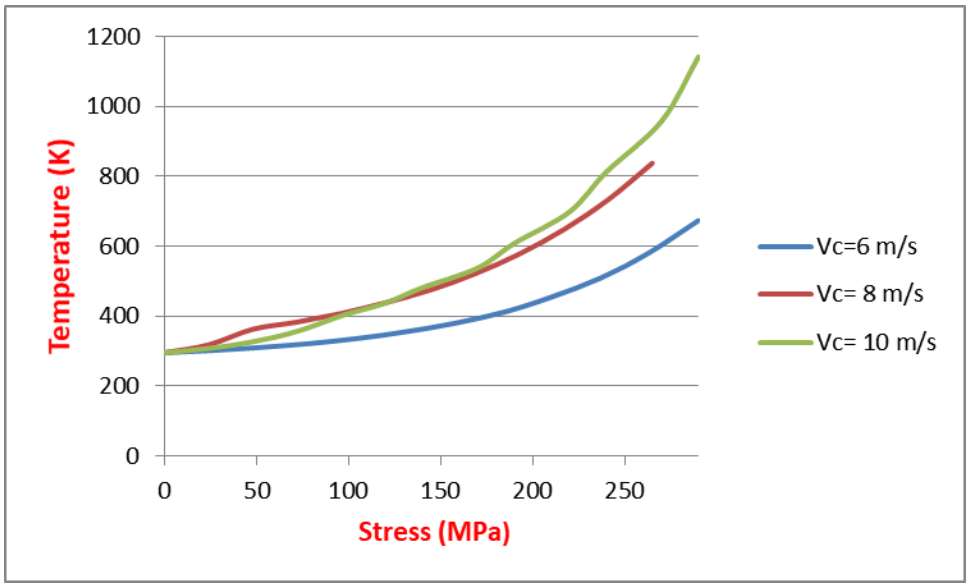


Figure (4.6) show the relation between the stress and the cutting temperature of Aluminum metal cutting at different cutting speed.

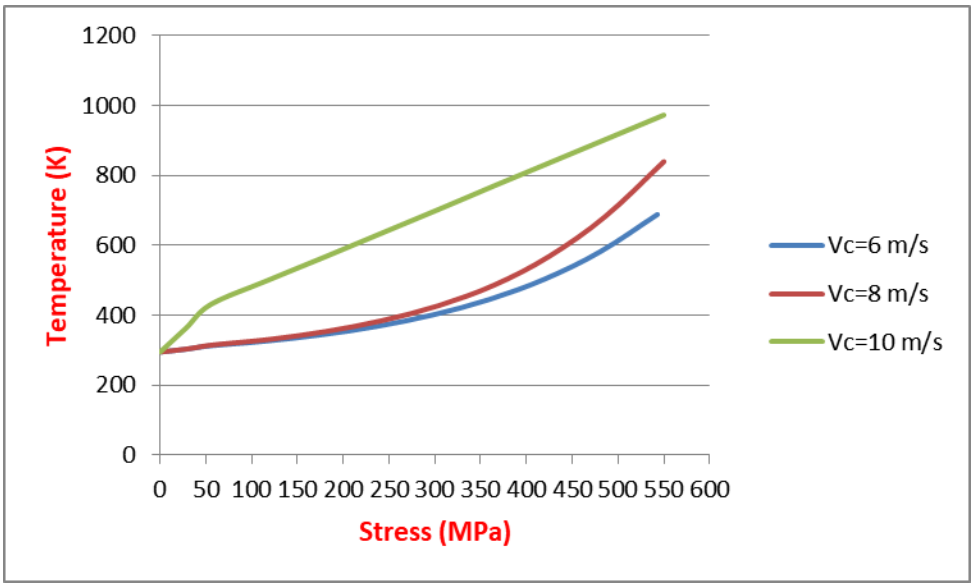


Figure (4.7) show the relation between the stress and the cutting temperature of Iron metal cutting at different cutting speed.

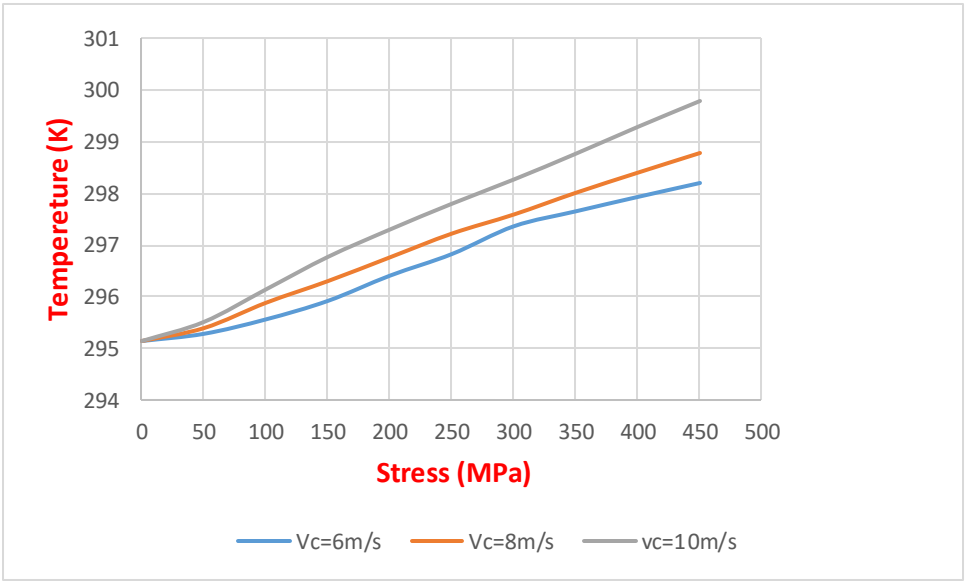


Figure (4.8) show the relation between the stress and the cutting temperature of Copper metal cutting at different cutting speed.

After the stresses generated in the cutting zones, the temperature generated in those zones are estimated at different cutting speed. Figure (4.9), (4.10) and (4.11) show the averge temperature distribution varying with time of (High speed steel, Carbide and Ceramic) cutting tool and (Aluminum, Iron and Copper) workpeice, respectively. At cutting speed varying from (6, 8 and 10) m/s. The results observed that a significant influence of cutting speed on the temperature generated in the machined models. As well as the time available for temperature dissipated decrease as the cutting speed increased.

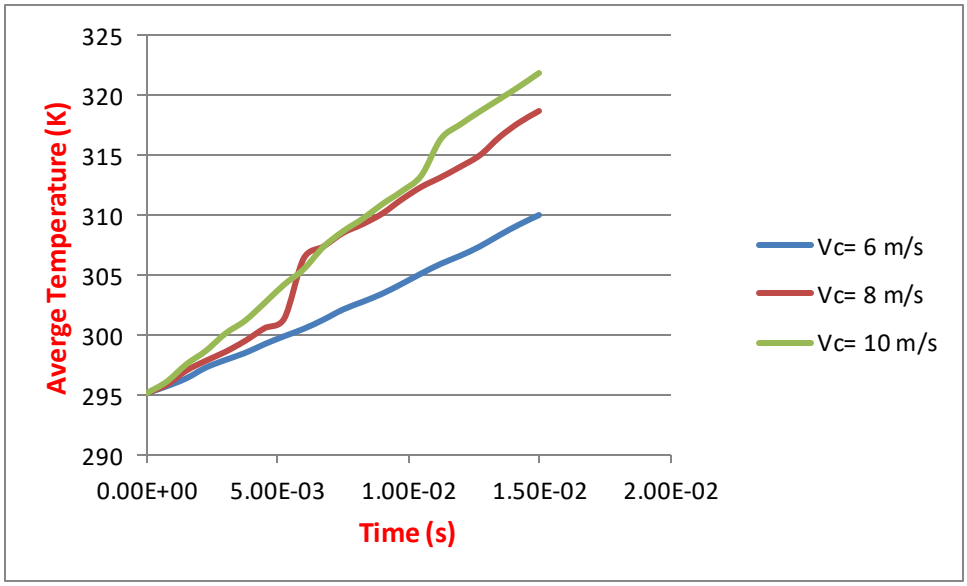


Figure (4.9) Show the average temperature varying with time of Aluminum metal cutting at different cutting speed.

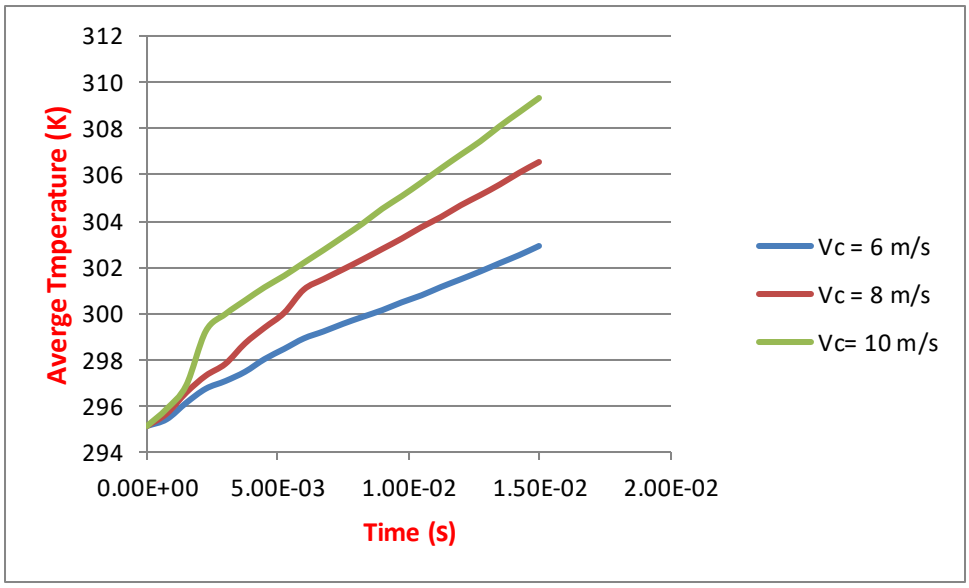


Figure (4.10) Show the average temperature varying with time of Iron metal cutting at different cutting speed.

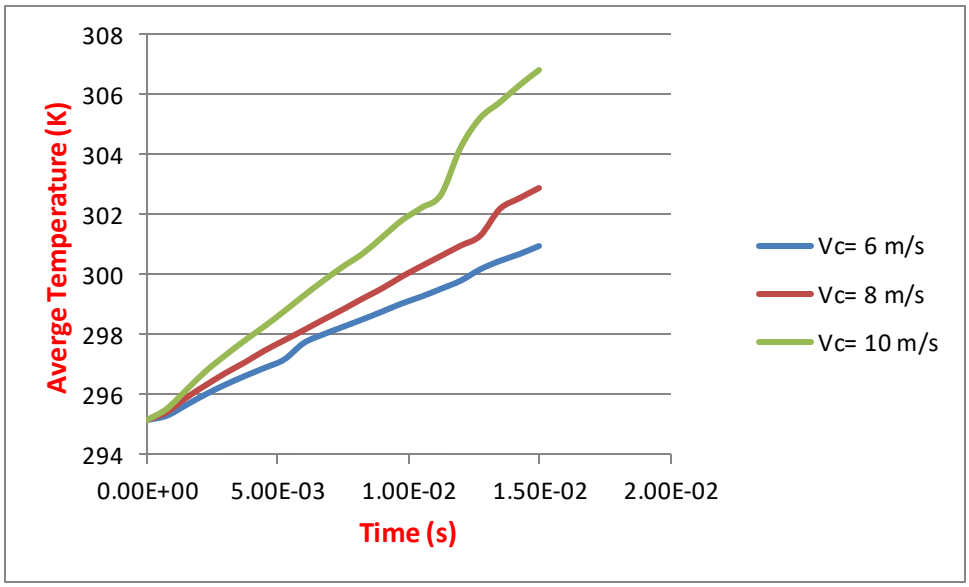


Figure (4.11) Show the average temperature varying with time of Copper metal cutting at different cutting speed.

Figures (4.12), (4.13) and (4.14) show contours of the temperature distribution at three different cutting speeds and depth of cuts for High Speed steel cutting tool and Aluminum workpeice. It can be seen that at DOC= 1.5 mm and cutting speed change from 6 m/s, 8 m/s and 10 m/s the maximum workpiece temperature increased from 673 K to 1141.4 K. Figures (4.15), (4.16) and (4.17) show contour of the temperature distribution at three different cutting speeds and depth of cuts for Carbide cutting tool and Iron workpeice. It seen that at DOC= 1.5mm and cutting speed from 6 m/s to 10 m/s the maximum workpiece temperature increased from 688.54 K to 972.98 K. Figures (4.18), (4.19) and (4.20) show contour of the temperature distribution at three different cutting speeds and depth of cuts for Ceramic cutting tool and Copper workpeice. It can be seen that at DOC= 1.5mm and cutting speed from 6 m/s to 10 m/s the maximum workpiece temperature increased from 535.49 K to 1099.7 K. So with the increasing of cutting speed, the temperature is increased. The reason for the increase in temperatures is due to the increased stresses formed in this area as a result of the increased cutting speed.

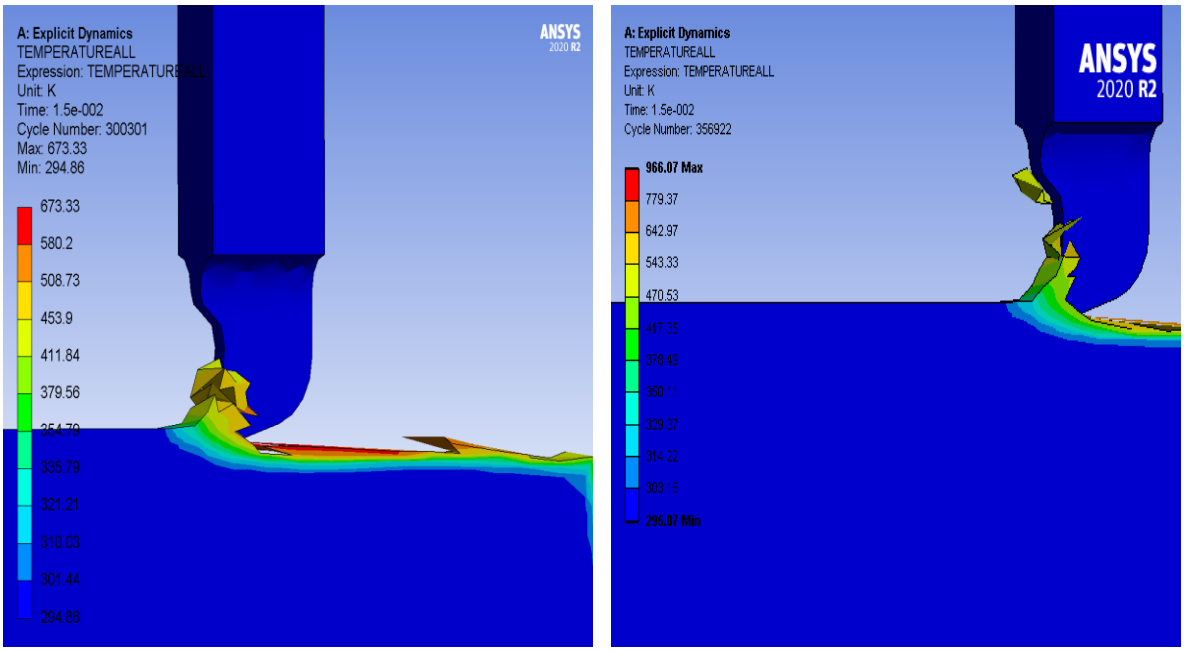


(a) (b)

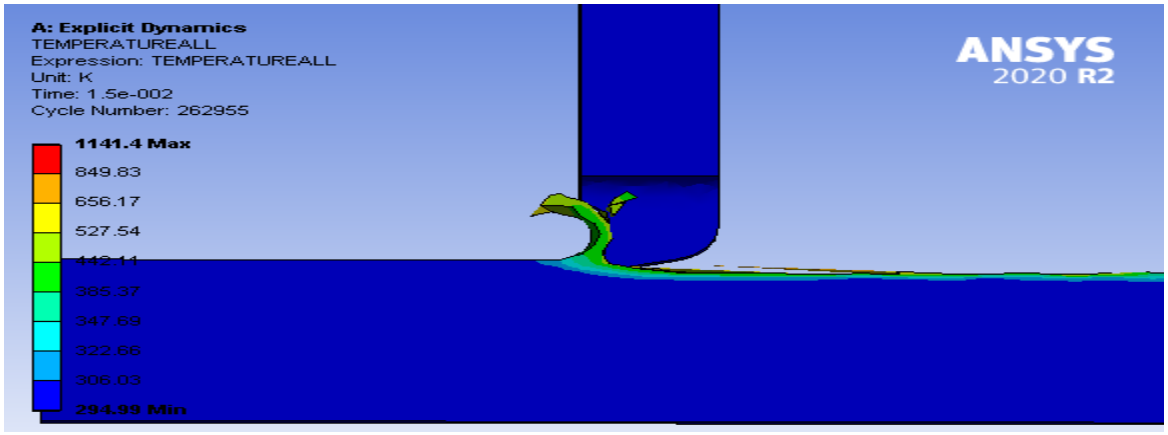


(c)

Figure (4.12) Show contours of cutting temperature distributions of HSS cutting tool and Aluminum workpeice at cutting depth=1.5 mm and (a) Vc= 6 m/s (b) Vc=8 m/s (c) Vc=10 m/s.

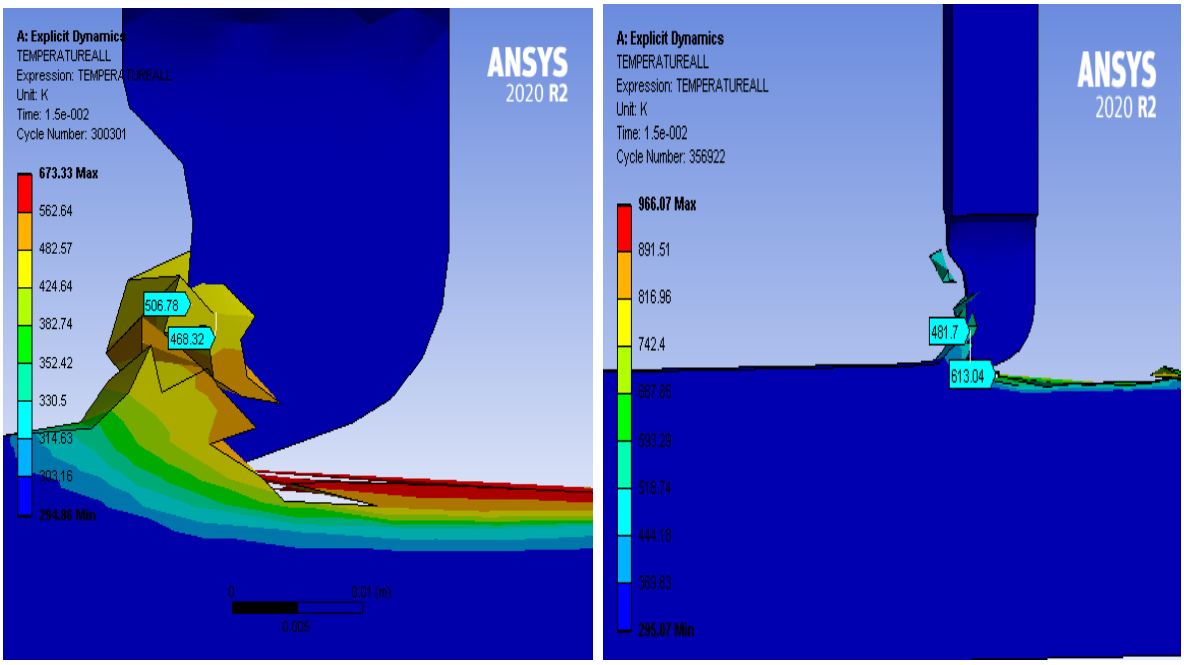


(a) (b)

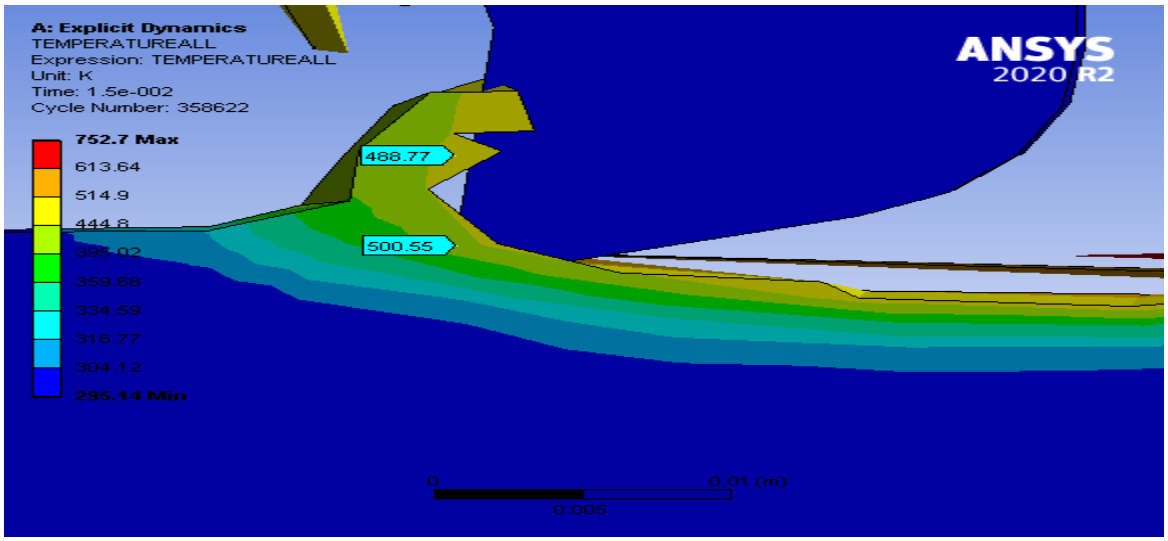


(c)

Figure (4.13) Show contours of cutting temperature distributions of HSS cutting tool and Aluminum workpeice at cutting depth=2 mm and (a) Vc= 6 m/s (b) Vc=8 m/s (c) Vc=10 m/s.

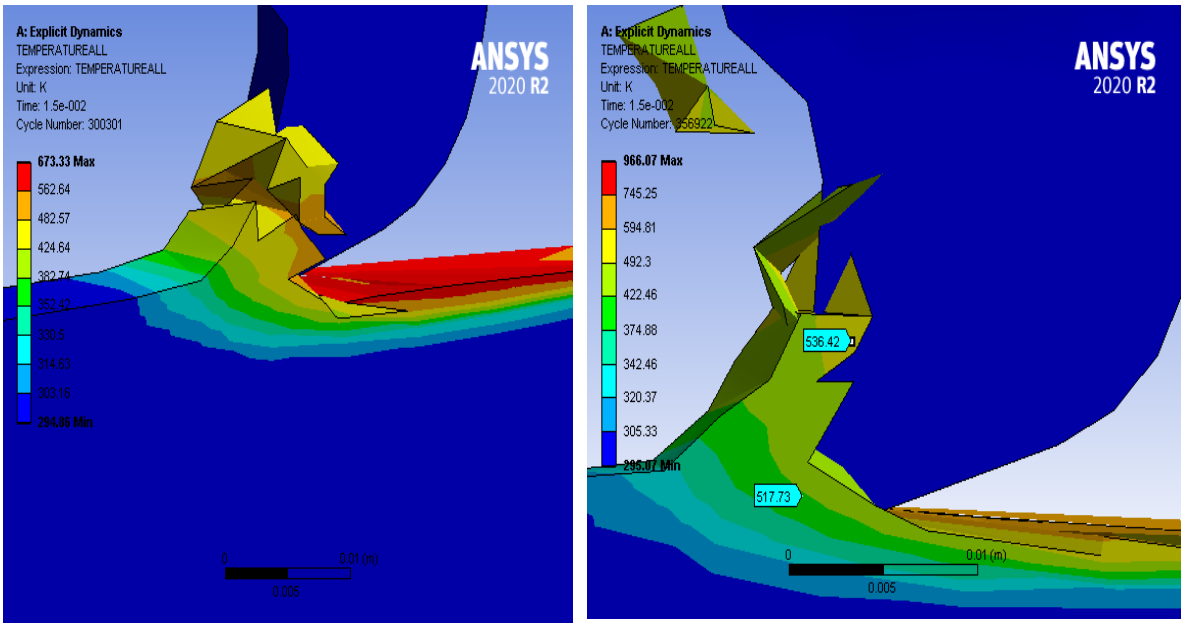


(a) (b)

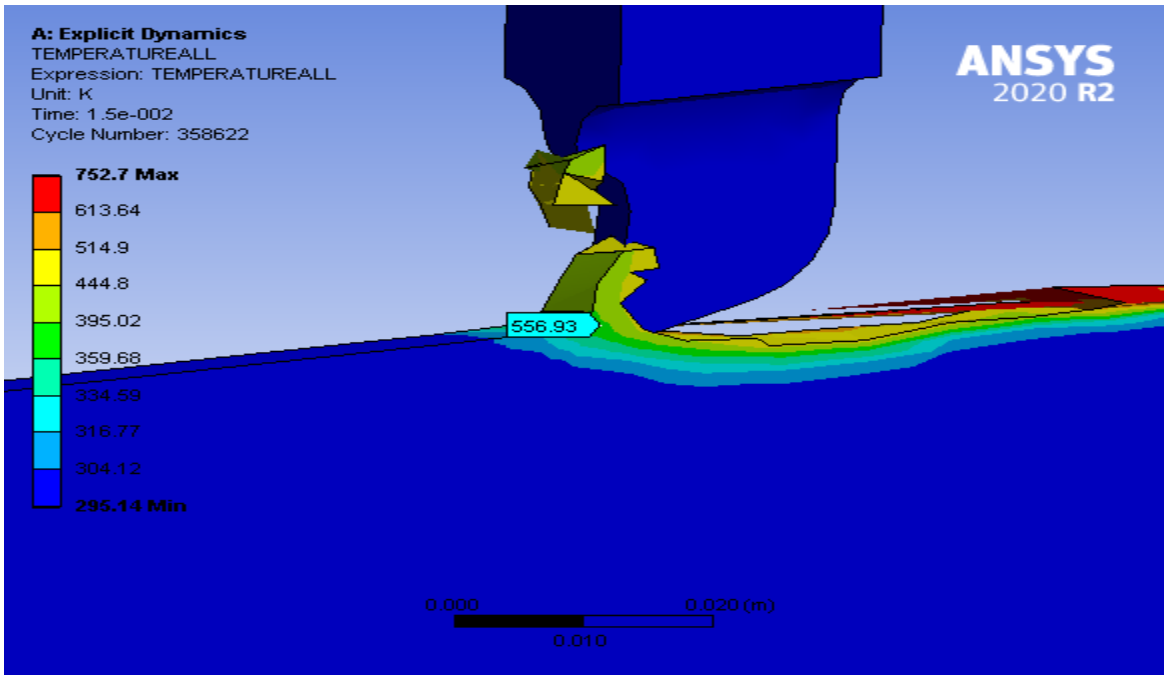


(c)

Figure (4.14) Show contours of cutting temperature distributions of HSS cutting tool and Aluminum workpeice at cutting depth= 2.5 mm and (a) Vc = 6 m/s (b) Vc= 8 m/s (c) Vc= 10 m/s.

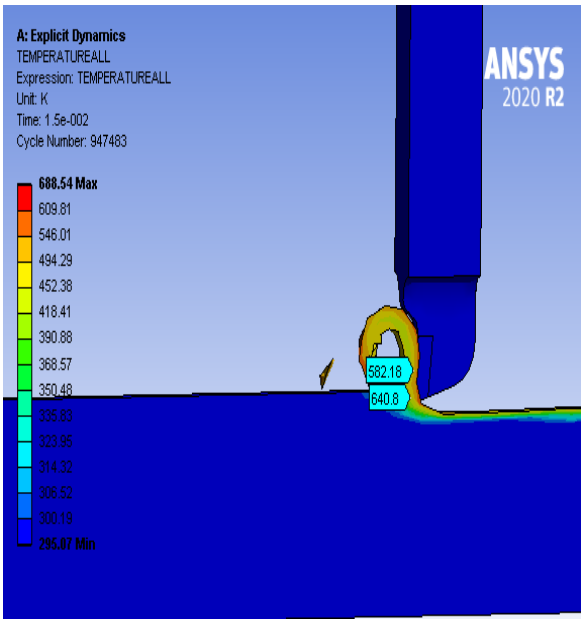


(a)

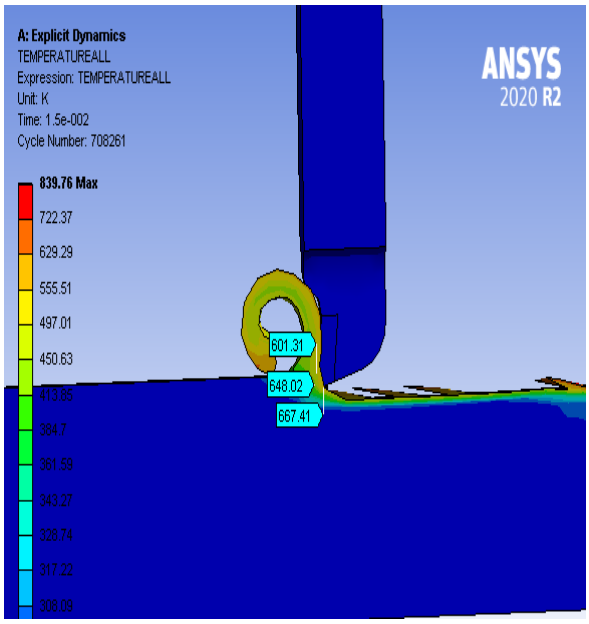


(b)

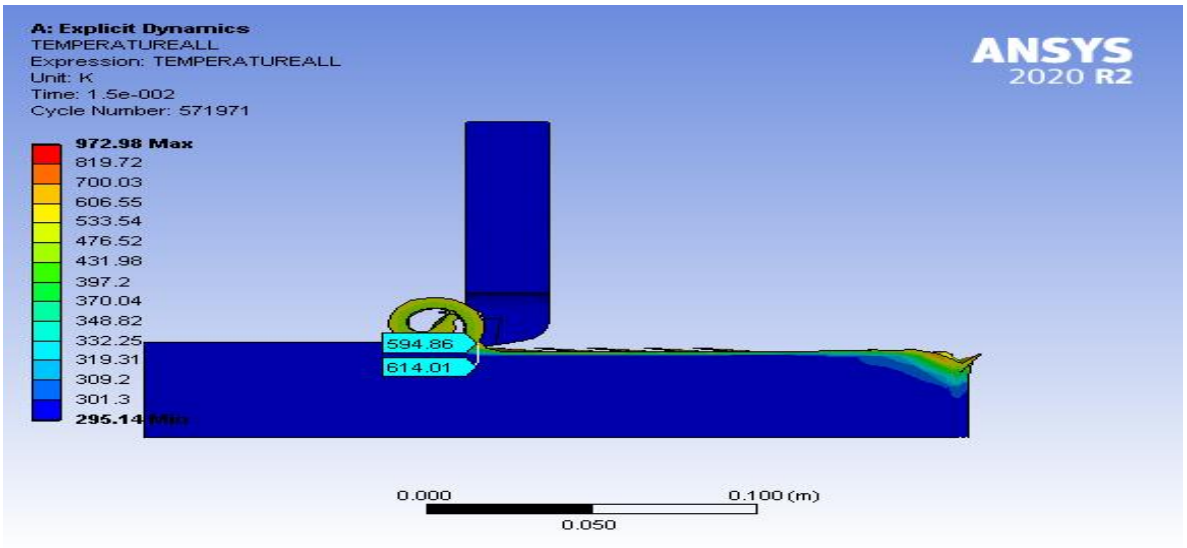


(c)

Figure (4.15) Show contours of cutting temperature distributions of Carbide cutting tool and Iron workpeice at cutting depth=1.5 mm and (a) Vc= 6 m/s (b) Vc=8 m/s (c) Vc=10 m/s.

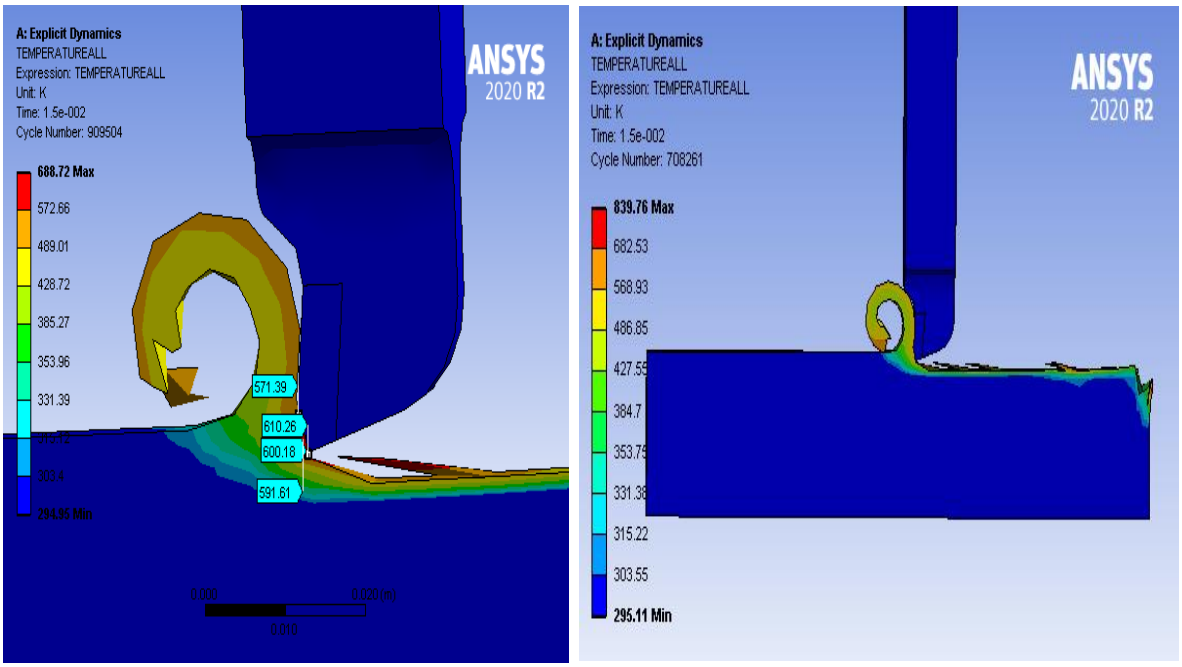


(a) (b)

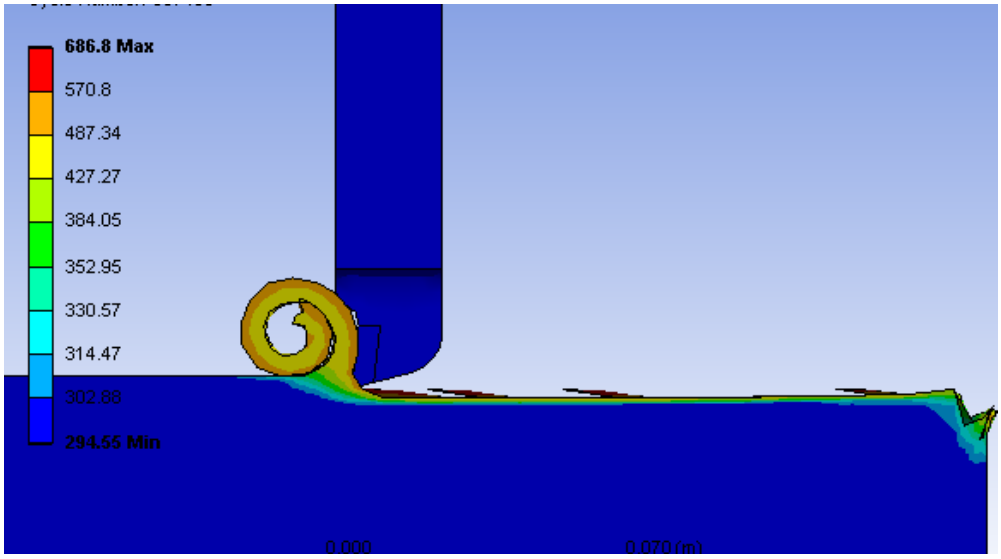


(c)

Figure (4.16) Show contours of cutting temperature distributions of Carbide cutting tool and Iron workpeice at cutting depth=2 mm and (a) Vc= 6 m/s (b) Vc=8 m/s (c) Vc=10 m/s.

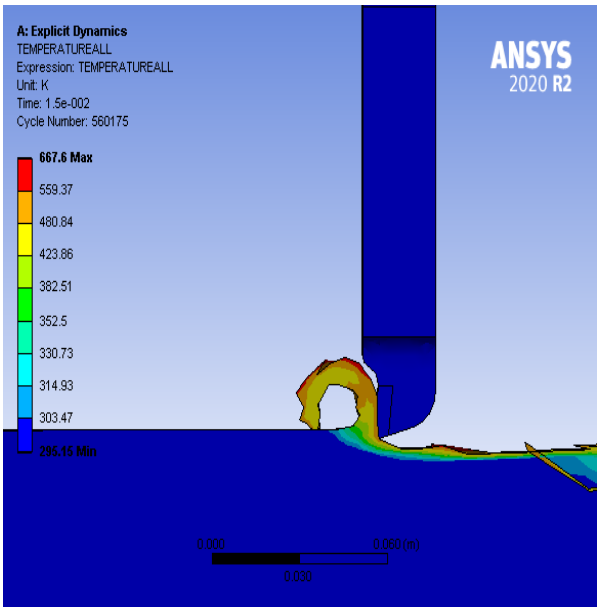


(a)

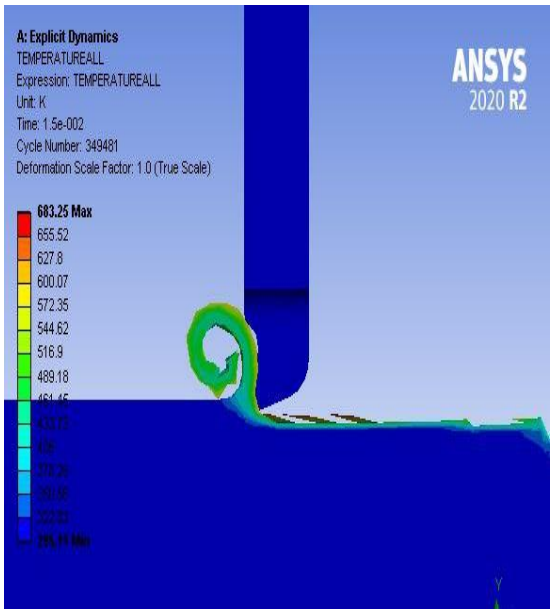


(b)

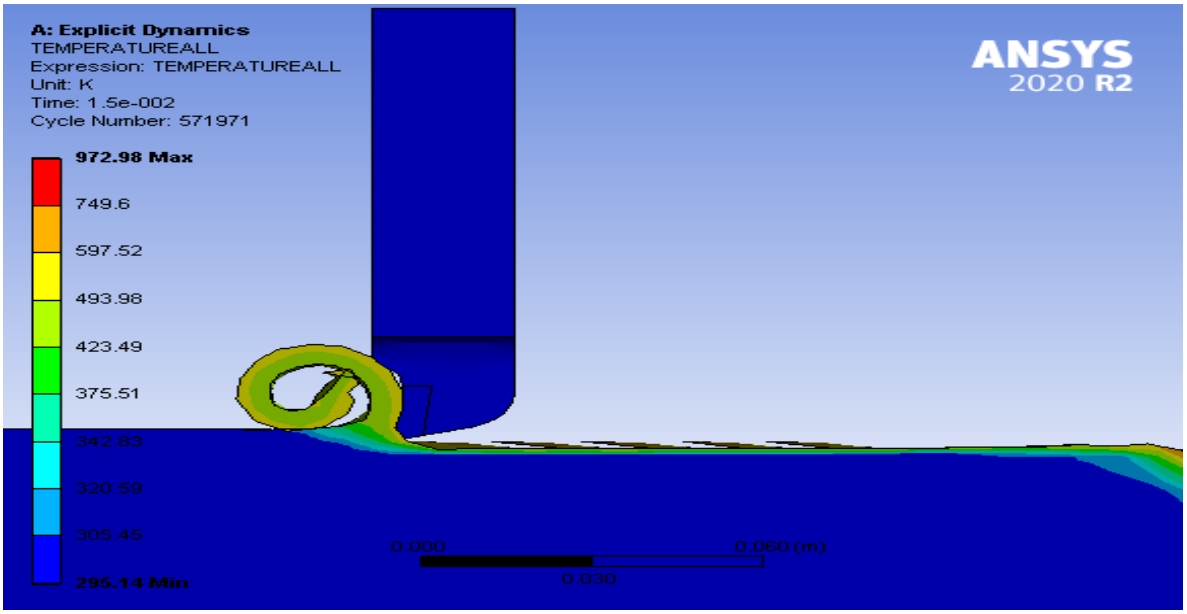


(c)

Figure (4.17) Show contours of cutting temperature distributions of Carbide cutting tool and Iron workpeice at cutting depth=2.5 mm and (a) Vc= 6 m/s (b) Vc=8 m/s (c) Vc=10 m/s.

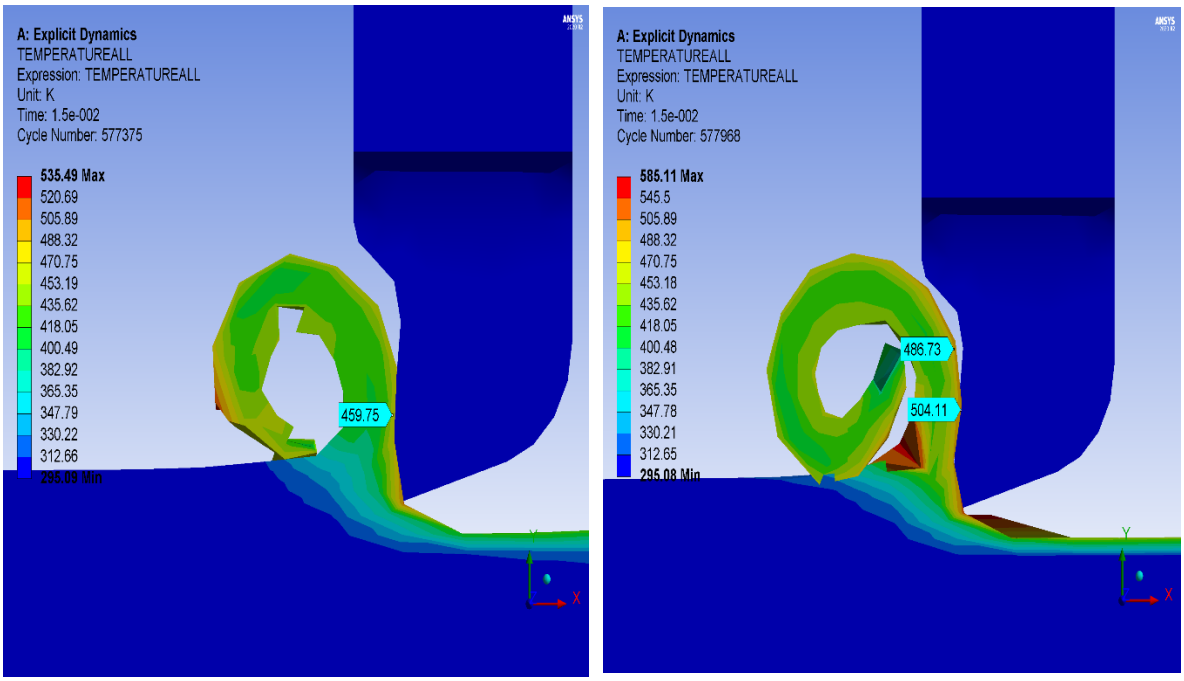


(a) (b)

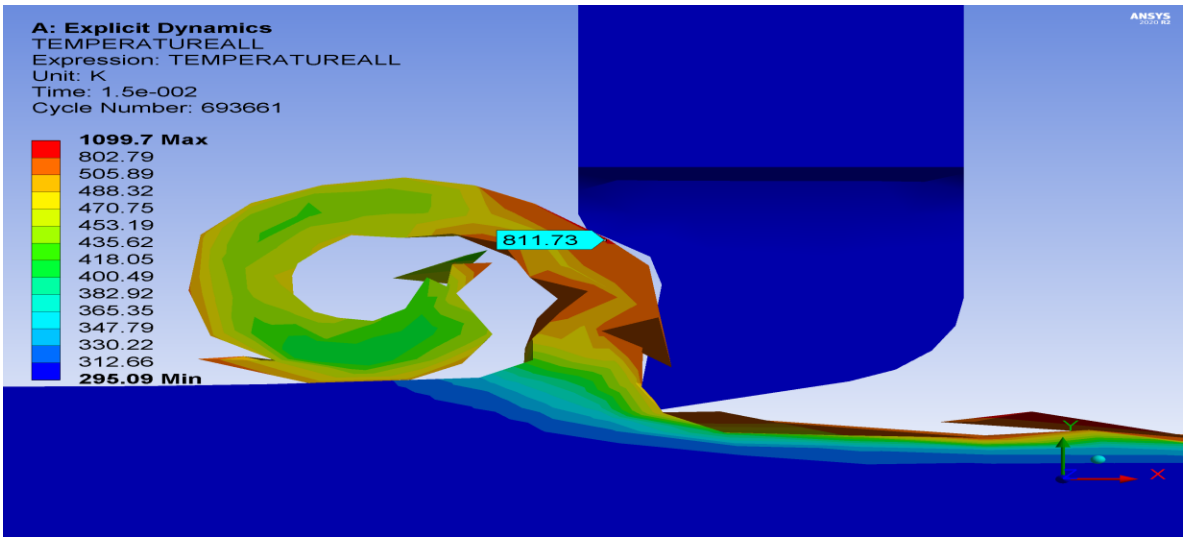


(c)

Figure (4.18) Show contours of cutting temperature distributions of Ceramic cutting tool and Copper workpeice at cutting depth=1.5 mm and (a) Vc= 6 m/s (b) Vc=8 m/s (c) Vc=10 m/s.

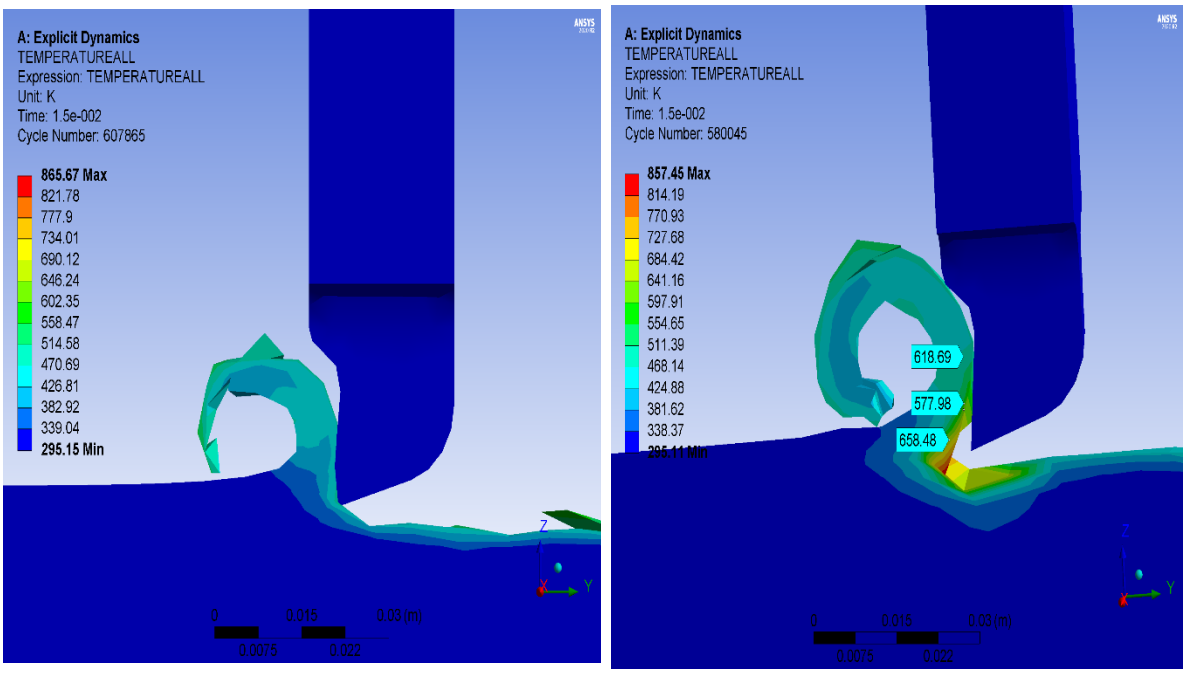


(a) (b)

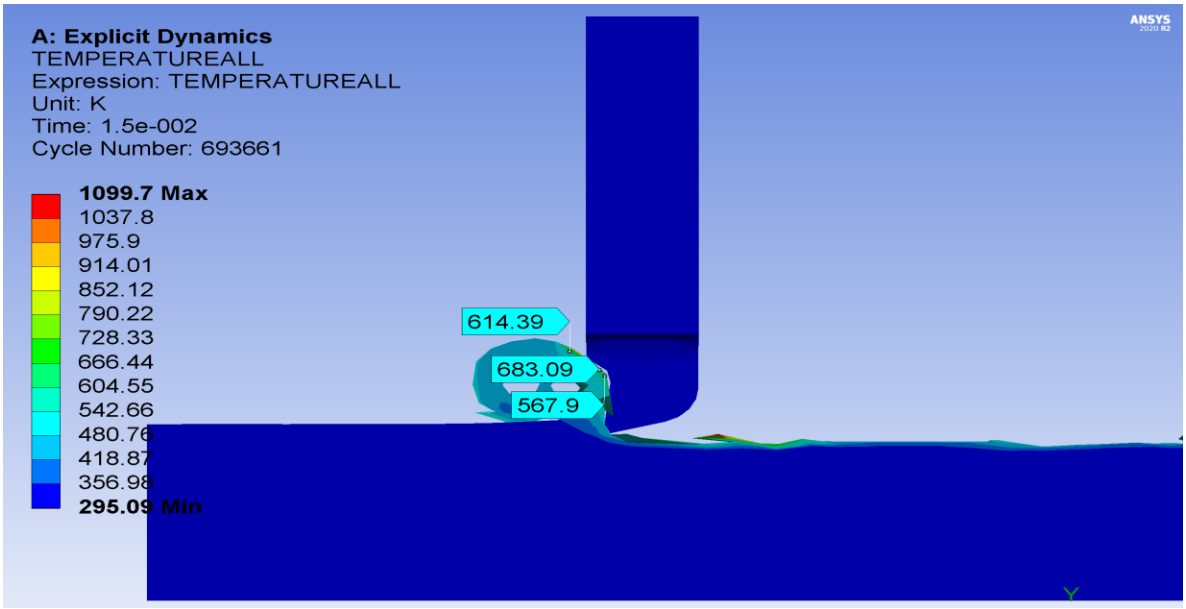


(c)

Figure (4.19) Show contours of cutting temperature distributions of Ceramic cutting tool and Copper workpeice at cutting depth=2 mm and (a) Vc= 6 m/s (b) Vc=8 m/s (c) Vc=10 m/s.

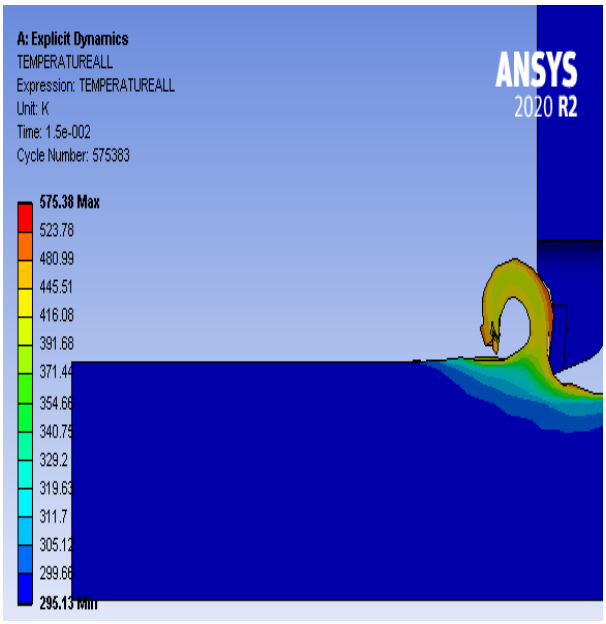


(a)

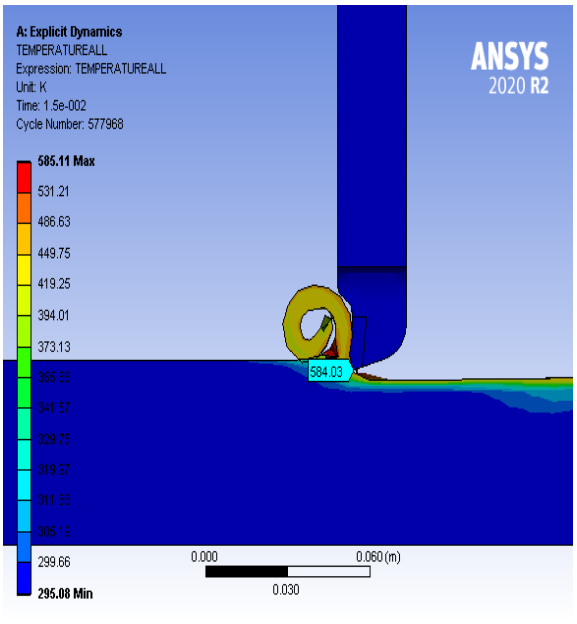


(b)

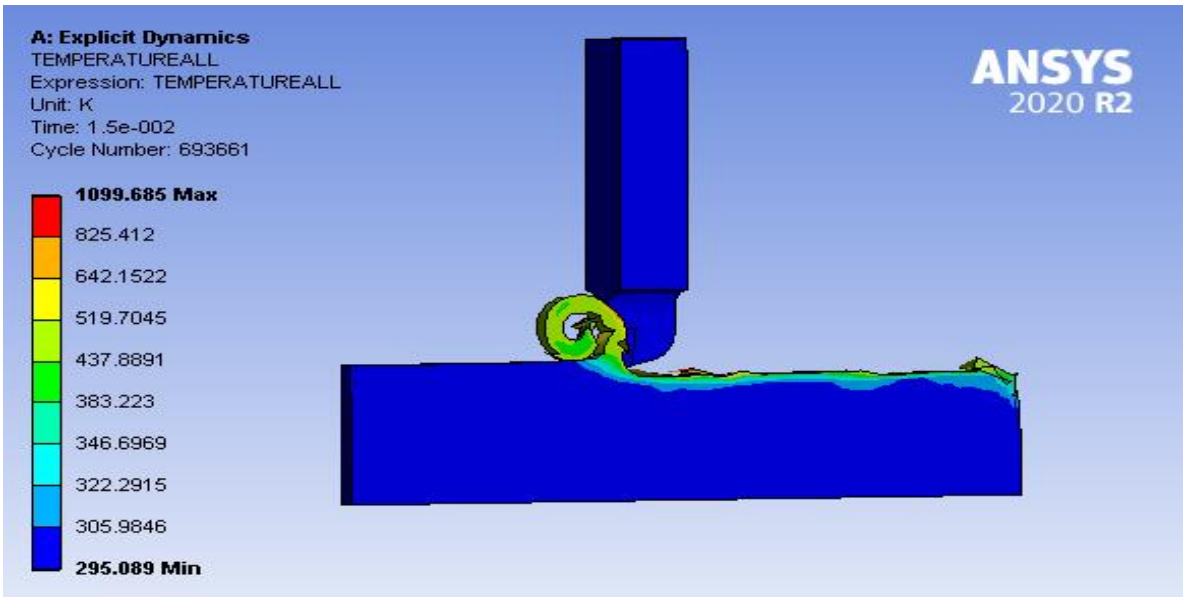


(c)

Figure (4.20) Show contours of cutting temperature distributions of Ceramic cutting tool and Copper workpeice at cutting depth=2.5 mm and (a) Vc= 6 m/s (b) Vc=8 m/s (c) Vc=10 m/s.

### 4.3.2 The Effect of Cutting Parameters on cutting Temperature

### A. Effect of cutting speed on temperature:

Cutting temperature is closely connected to cutting speed. With increase of cutting speed, friction increases, this induces an increase in temperature in the cutting zone. Figure (4.21) shows the effect of cutting speed on the cutting temperatures (chip-tool interface temperature) for High speed steel cutting tool and Aluminum workpeice. So the cutting speed 6 m/s at the chip-tool interface temperature is 446.16 K and when cutting speed increases to 8 m/s the temperature increases to 471.52 K in cutting zone also when cutting speed increases to 10 m/s the temperature increases to 486.91 K. The same trend was obtained for different depth of cut values of 1.5 mm and 2.5 mm. So it can be seen that the temperature at chip-tool interface is increase with the cutting speed increasing. Figure (4.22) shows the effect of cutting speed on the cutting temperatures (chip-tool interface temperature) for (Carbide, Iron) cutting tool and workpeice respectively. Figure (4.23) shows the effect of cutting speed on the cutting temperatures (chip-tool interface temperature) for Ceramic cutting tool and Copper workpeice.

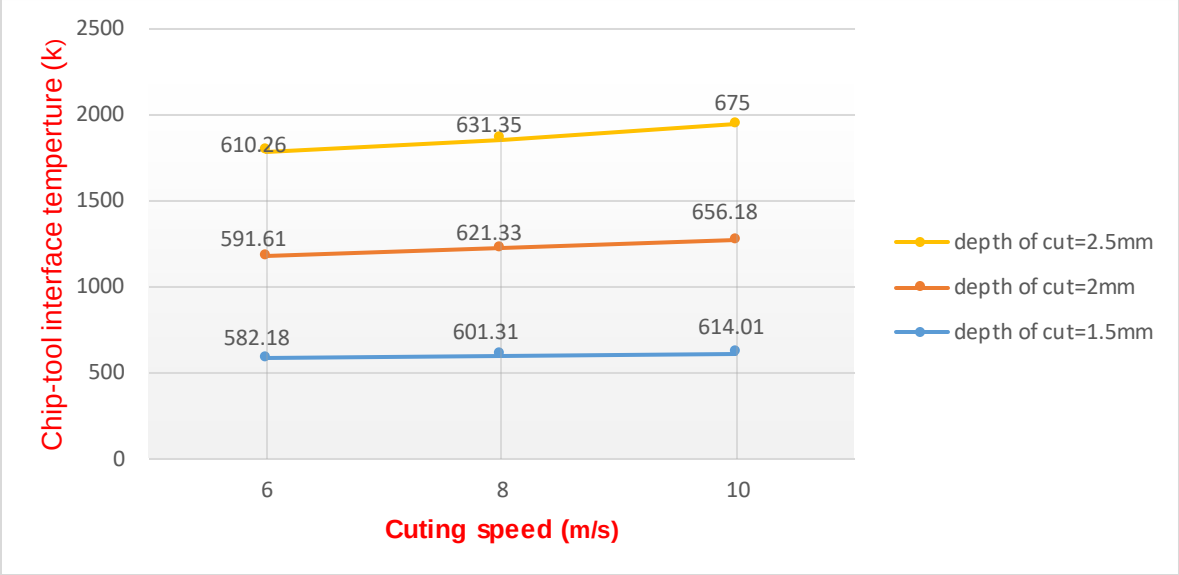


Figure (4.21) shows the effect of cutting speed on the cutting temperatures (chip-tool interface temperature) for HSS- tool and Al-workpeice.

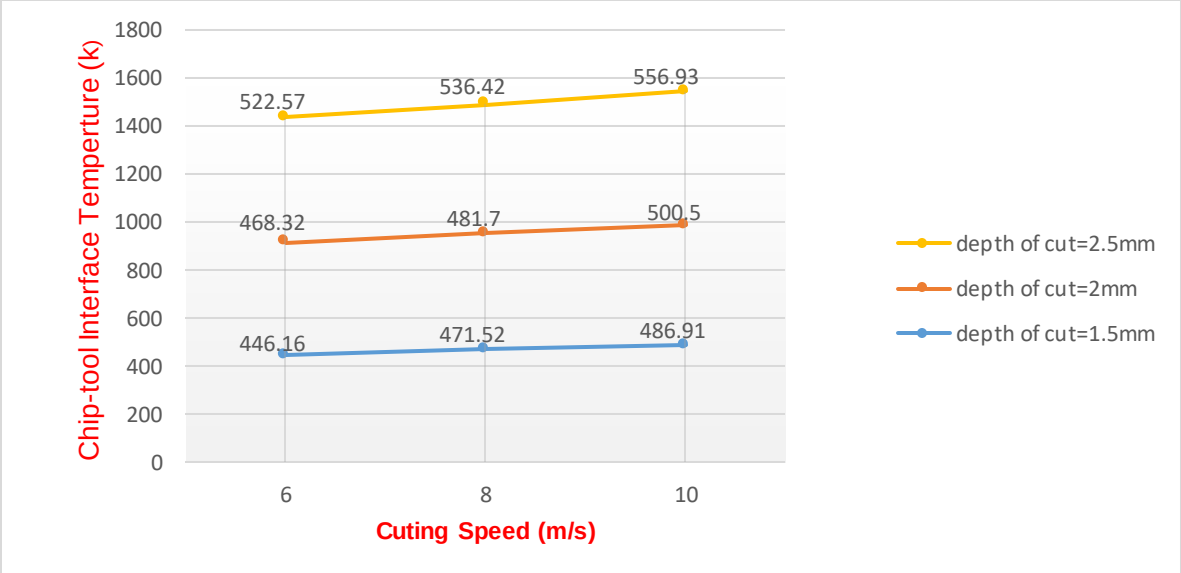


Figure (4.22) shows the effect of cutting speed on the cutting temperatures (chip-tool interface temperature) for Carbide cutting tool and Iron workpeice.

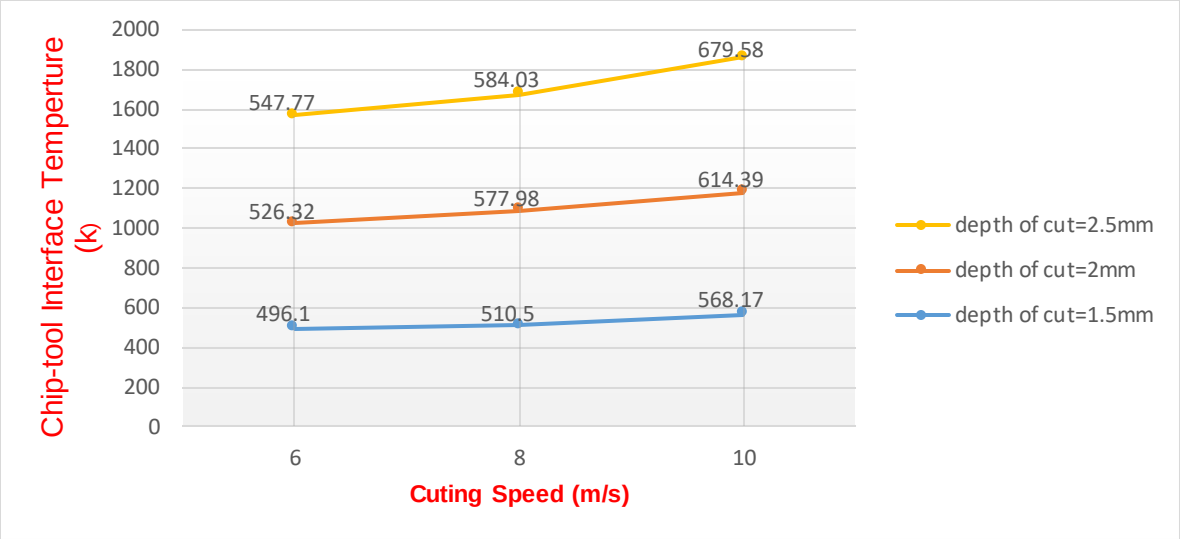


Figure (4.23) shows the effect of cutting speed on the cutting temperatures (chip-tool interface temperature) for Ceramic cutting tool and Copper workpeice.

It can be noticed from the graphs that the temperature at the chip-tool interface increases with the increase in the cutting speed, even with the difference in the type of metal of the cutting tool and the workpiece.

## B) Effect of depth of cut on cutting temperature

Figures (4.24), (4.25) and (4.26) show the change of the cutting temperature obtained in cutting zone as the function of depth of cut with respect to different cutting speed and material type of tool and workpeice. It seen for the depth of cut 1.5 mm, the recorded temperature is 446.16 K when the depth of cut increases to 2 mm the value of temperature becomes 468.32 K. And when the depth of cut increases to 2.5 mm, the value of temperature becomes 522.57 K. So if the depth of cut increases, the section of chip increases and friction of chip-tool increases what leads to an increase in temperature.


Figure (4.24): show the effects of cutting depth on chip-tool interface temperature for High speed steel tool and Aluminum-workpeice.

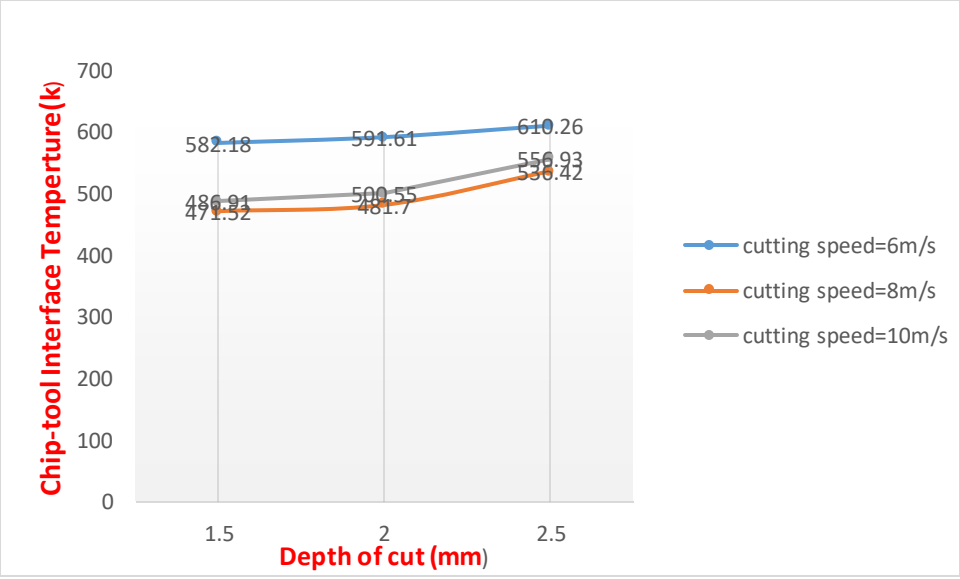


Figure (4.25): Show the effect of cutting depth on chip-tool interface temperature for Carbide cutting tool and Iron workpeice.

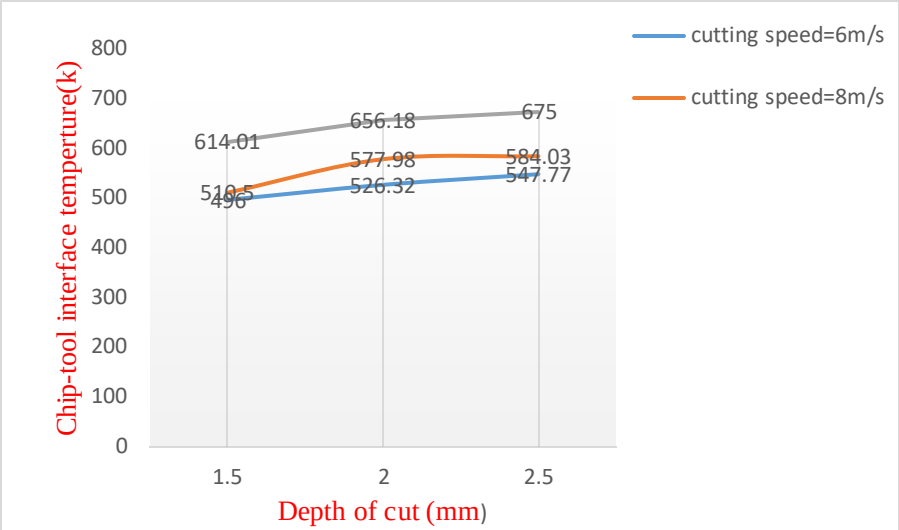


Figure (4.26): Show the effect of cutting depth on chip-tool interface temperature for Ceramic cutting tool and Copper workpeice.

### 4.3.3 Temperature distributions in the cutting tool:

In the cutting process the tool is move with the constant velocity and the workpeice is fixed as the cutting process is started both the workpeice and cutting tool temperature are increased. Thus for more accurate simulation a natural force convection have been consideres in the modeling of case study. It considered the coefficient of heat convection for tool and chip is 26 $w/m^2$ .k. And for workpeice is 8 $w/m^2$.k.

### 4.3.3.1 Temperature contours inside the cutting tool

Figure (4.27) show the temperature gradient inside the cutting tool on YZ plane. It can be seen clearly that maximum temperature appears at the interface of the tool tip then it gradually decrease away from the tool tip. Figure (4.28) shows a planes inside the tool on the plane YZ. It noted that the maximum temperature is 554.8 K at 252.2 mm distance from tool tip while the temperature was 544.5 K at 254.3 mm distance and at 254.3 mm from tool tip the maximum

temperature will be less. Thus, the further away from the source of heat the temperature was decrease.

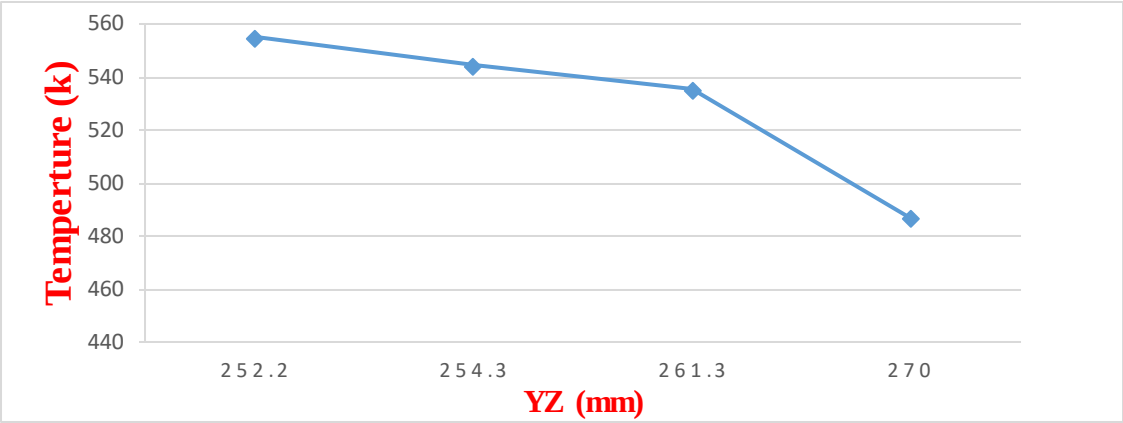


Figure (4.27) show the temperature gradient inside the cutting tool on YZ plane.

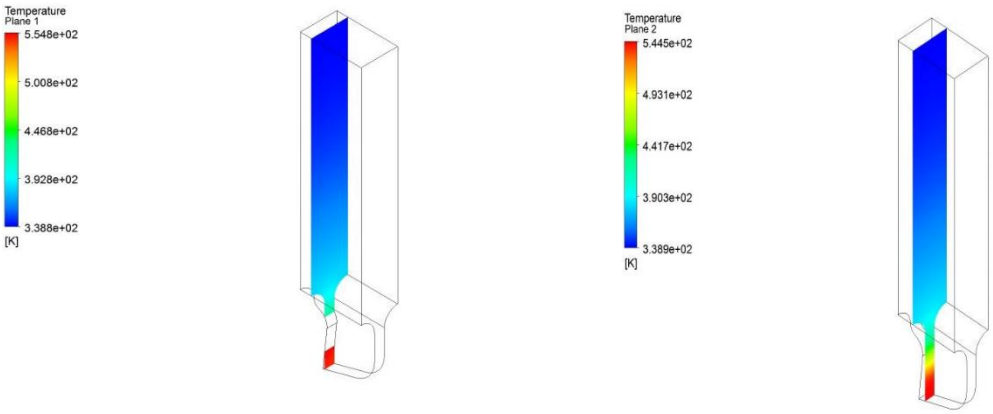


(a) (b)

Fig (4.28): Temperature distribution contours inside cutting tool on plane YZ at (a) h=252.2 mm (b) h= 254.3 mm

Likewise, it seen this distribution of temperature inside the tool on planes ZX and XY. It proved the temperature is gradually decreases keep away from the heat source. Figures (4.29) and (4.30) show graphically the temperature gradient inside the cutting tool on ZX and XY planes. Figures (4.31) and (4.32) show the temperature distribution contours inside cutting tool on ZX and XY planes.

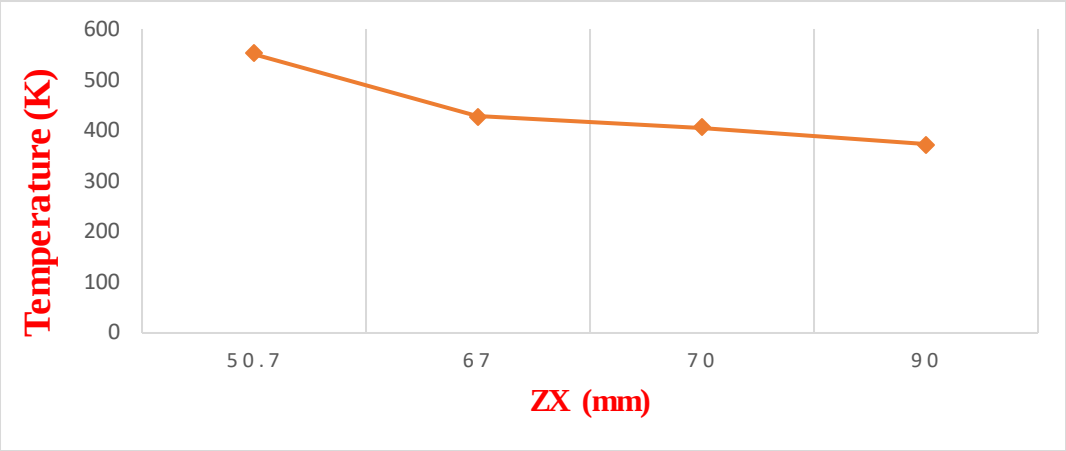


Figure (4.29) Show the temperature gradient inside the cutting tool on ZX plane.

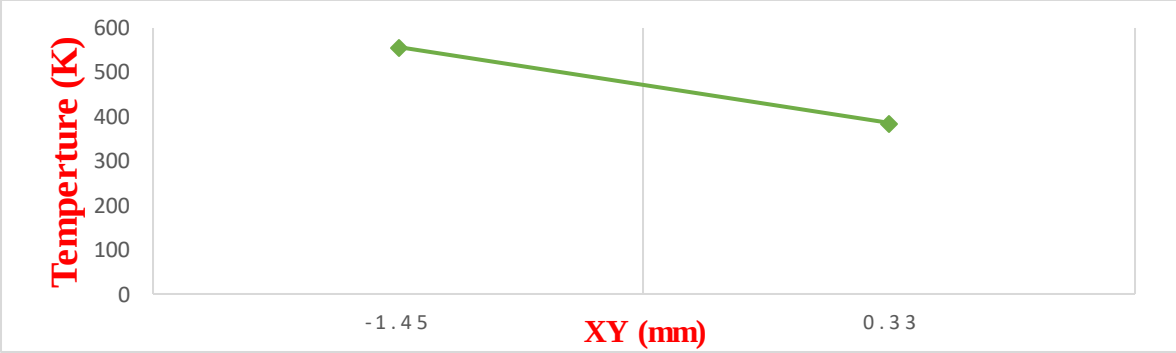


Figure (4.30) Show the temperature gradient inside the cutting tool on XY plane.

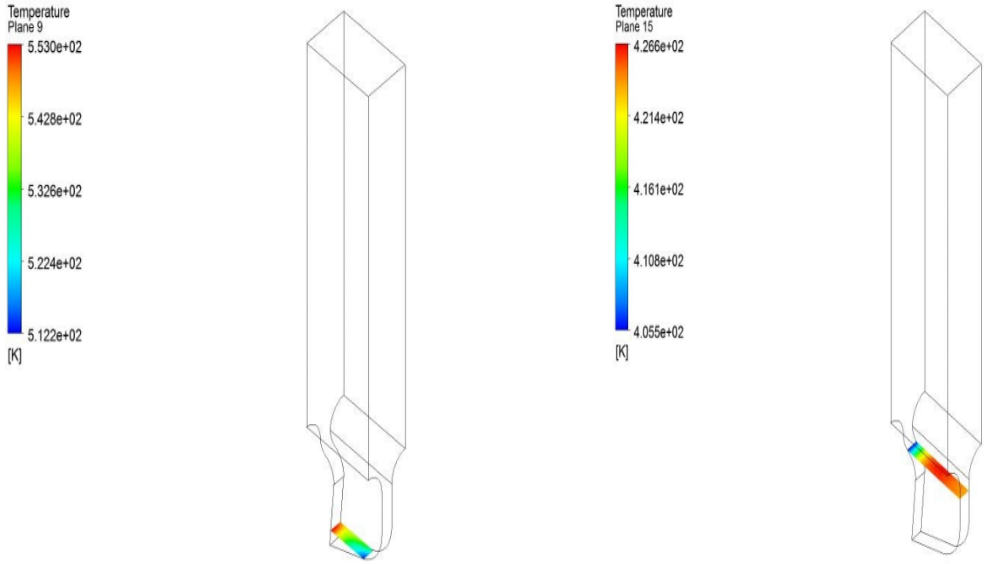


(a) (b)

Figure (4.31): Show temperature distribution contour inside cutting tool on ZX plane at (a) h=50.7 mm (b) h= 67.0 mm.

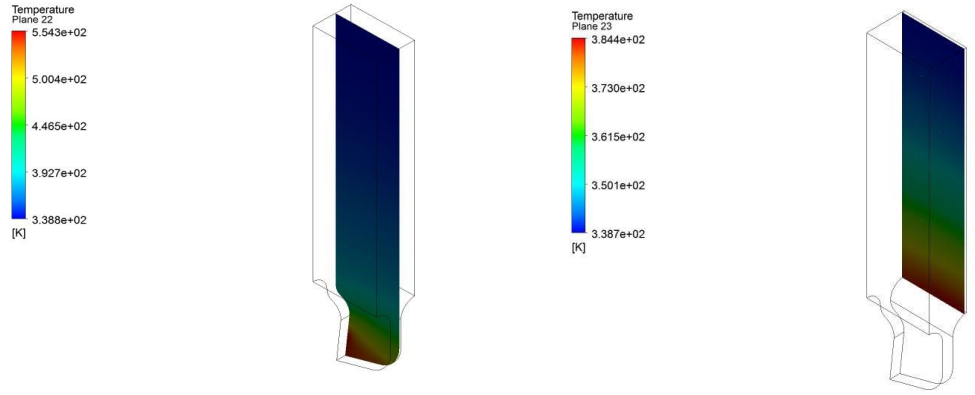


(a) (b)

Figure (4.32): Show temperature distributions contours inside cutting tool on XY plane at (a) h= - 1.45 mm (b) h= 0.33 mm

### 4.3.3.2 Three dimensional Temperature distributions in the cutting tool insert:

The temperature of cutting tool can be estimated by ANSYS/Fluent. Generally, the temperature in the cutting tools is lower than the temperature resided in chips. This can be ascribed to following two aspects. Firstly, the chips experience not only the intensive friction but also the plastic deformation generated by the extrusion of cutting tools. But the cutting tools only undergoes the friction resulted from the chips and work piece due to its higher hardness than workpiece. Additionally, the thermal contact conductance of tool-chip interface affects heat transfer; thus, the cutting heat transferred to the cutting tools is reduced. After applying the boundary conditions on the cutting tool, Figure (4.33) show the temperature contours of High Speed steel cutting tool and aluminum work material. Figure (4.34) show the temperature contours of Carbide cutting tool and Iron work material. Figure (4.35) show the temperature contours of Ceramic cutting tool and Copper work material. It is indicated that the maximum temperature appeared at the connection surface between the insert and the workpiece where the heat flux effects directly on the insert. It can be shown that most of the body of cutting holders have temperature equals to 300 K and this means that the heat does not reach all the regions of the holder. It is seen that the heat transfer by conduction through the insert and then to the tool holder. The heat transferred by convection from the outer surfaces to the surrounding leads to reduce the temperature of the body of the holder. At the

start, the tooltip was warmed by the applied heat flux, and then with the time spending, the thermal energy is dispersed in the tool.

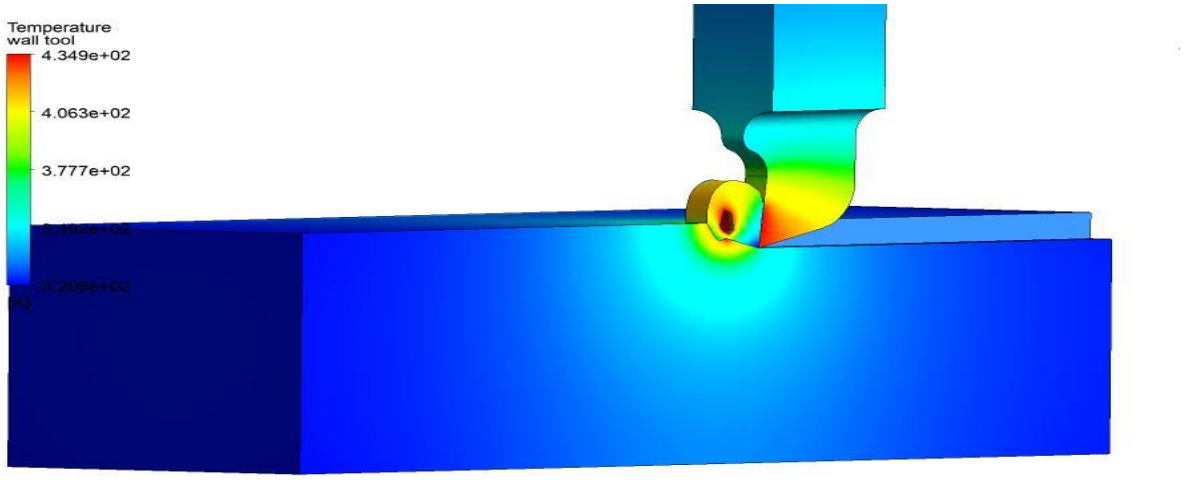


Figure (4.33) show the temperature contours of High Speed steel cutting tool and aluminum work material.

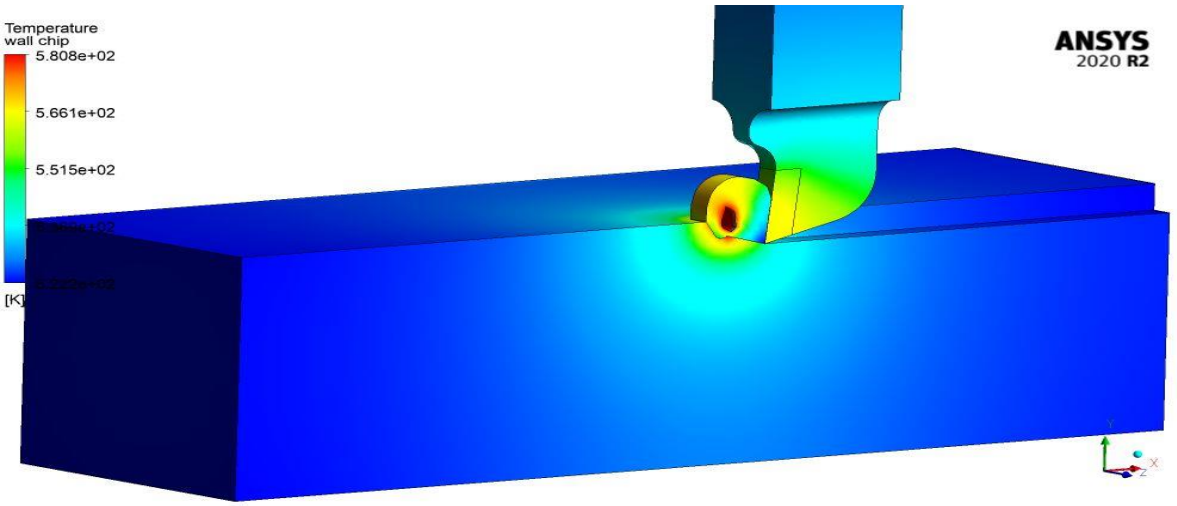


Figure (4.34) show the temperature contours of Carbide cutting tool and Iron work material.

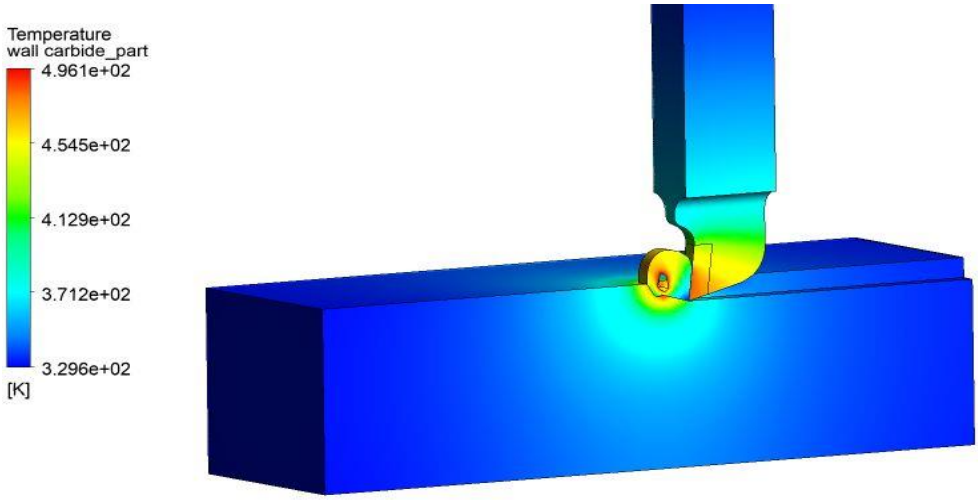


Figure (4.35) show the temperature contours of Ceramic cutting tool and Copper work material.

# *CHAPTER FIVE*

# *CONCLUSIONS AND RECOMMENDATIONS*

# CHAPTER FIVE

# CONCLUTIONS AND RECOMMENDATIONS FOR FUTURE WORK

## 5.1 CONCLUTIONS

This work involving two major areas of mechanical engineering: heat transfer and manufacturing processes. Based on the knowledge of these two areas, a new computational algorithm for solving problems of heat transfer applied to manufacturing processes.

This work studied the thermal effects during cutting process and also analyzes the influence of the cutting conditions (cutting speed and depth of cut) on the temperature generated at cutting zone.

Based on the method used in this study the following conclusions regarding our approach to temperature modeling could be made.

I. Finite element method using ANSYS / Explicit Dynamic program is found to be a successful technique to perform trend analysis to estimate cutting temperatures in metal cutting with respect to various combinations of design variables (metal cutting speed and depth of cut).
II. The results from FE simulations show that the friction has a strong influence on chip geometry and cutting temperature.
III. The minimum temperatures were attained at a cutting speed of 6 m/s and cutting depth 1.5 mm.

IV. The maximum temperatures were achieved at a cutting speed of 10 m/s and depth of cut 2.5 mm.

V. The higher percentage of increase in Aluminum workpiece temperature owing to the increase of cutting speed is 8.36 %, when transferring from 6 m/s to 10 m/s at cutting depth of 1.5 mm. While the higher percentage of increase in Iron workpiece temperature is 9.84 %, also when cutting speed transferring from 6 m/s to 10 m/s at cutting depth 2 mm. And for Copper workpeice the higher percentage of increase in temperature is 19.39%, also when cutting speed transferring from 6 m/s to 10 m/s at cutting depth 2.5 mm. This means that the influence of the speed on the amount of maximum temperature generated in the machined model is found to increase significantly with increase of cutting speed.

VI. The temperature field in any region of the tool set (insert and tool-holder) is calculated from the temperatures estimation at the cutting interface.

VII. For high-speed steel as the tool insert material, the maximum temperature is 537.14 K, and for Carbide and Ceramic are 602.31 K and 661.72 K respectively.

VIII. Maximum temperature were found at the tool tip then it gradually decrease away from the tool tip.

## 5.2 Suggestion for Future Work

1. Studying the effect of different cutting fluid on heat distribution in the cutting tool with comparison with dry cutting.
2. Studying the effect of thin coating of hard material like (TiN, TiC) on tool surface on heat generated during cutting.
3. In this study, the numerical analysis is used, so we can done experimental work and comparing with the numerical results.

## References


[1] Salodkar, S. M. (2022), "Development of Tool Chip Interface Temperature Detection System for the Investigation of Temperature during Machining of Alloy Steel", Journal of Algebraic Statistics, 13(3), 1593–1606.

[2] M. A. Habib, “Analytical Modeling of Cutting Force and Cutting Temperature in Turning Steel Under Cryogenic,” Bangladesh University Of Engineering & Technology, Thesis, no. December, 2013.

[3] C. Kilicaslan, “Modelling and Simulation of Metal Cutting By Finite Element Method,” İzmir Institute of Technology, Thesis, no. December, 2009.

[4] Coskun Islam, " A Transient Thermal Model for Machining", The University of British Columbia, Thesis,no. October,p. 2018, 2018.

[5] Komanduri, R. (2001). "A review of the experimental techniques for the measurement of heat and temperatures generated in some manufacturing processes and tribology", *Tribology International*, *34*(10), 653–682. https://doi.org/10.1016/S0301-679X(01)00068-8

[6] Kus, A., Isik, Y., Cemal Cakir, M., Coşkun, S., & Özdemir, K. (2015), "Thermocouple and infrared sensor-based measurement of temperature distribution in metal cutting", Sensors (Switzerland), *15*(1), 1274–1291. https://doi.org/10.3390/s150101274

[7] Abukhshim, N. A., Mativenga, P. T., & Sheikh, M. A. (2006),"Heat generation and temperature prediction in metal cutting",A review and implications for high speed machining. International Journal of Machine Tools and Manufacture, *46*(7–8), 782–800. https://doi.org/10.1016/j.ijmachtools.2005.07.024

[8] P. Kuriakose, “Thermal Analysis of Single Point Cutting Tool,” Cochin University of Science And Technology, Thesis, pp. 1–79, 2014.

[9] Jen, T. C., Gutierrez, G., & Eapen, S. (2001)," Numerical analysis in interrupted

cutting tool temperatures," Numerical Heat Transfer; Part A: Applications, 39(1), 1–20. https://doi.org/10.1080/10407780117053

[10] Majumdar, P., Jayaramachandran, R., & Ganesan, S. (2005). "Finite element analysis of temperature rise in metal cutting processes," Applied Thermal Engineering,25(14–15),2152–2168. https://doi.org/10.1016/j.applthermaleng.2005.01.006

[11] Carvalho, S. R., Lima e Silva, S. M. M., Machado, A. R., & Guimarães, G. (2006)," Temperature determination at the chip-tool interface using an inverse thermal model considering the tool and tool holder," Journal of Materials Processing Technology, 179(1–3), 97–104. https://doi.org/10.1016/j.jmatprotec.2006.03.086

[12] Grzesik, W. (2006)," Determination of temperature distribution in the cutting zone using hybrid analytical-FEM technique," International Journal of Machine Tools and Manufacture, 46(6), 651–658. https://doi.org/10.1016/j.ijmachtools.2005.07.009

[13] Zhang, S., & Liu, Z. (2008)," An analytical model for transient temperature distributions in coated carbide cutting tools," International Communications in Heat and Mass Transfer, 35(10), 1311–1315. https://doi.org/10.1016/j.icheatmasstransfer.2008.08.001

[14] Kadirgama, K., Noor, M. M., Rahman, M. M., Harun, W. S. W., & Haron, C. H. C. (2009)," Finite element analysis and statistical method to determine temperature distribution on cutting tool in end-milling," European Journal of Scientific Research, 30(3), 451–463.

[15] Ulutan, D., Lazoglu, I., & Dinc, C. (2009)," Three-dimensional temperature predictions in machining processes using finite difference method," Journal of Materials Processing Technology, 209(2), 1111–1121. https://doi.org/10.1016/j.jmatprotec.2008.03.020

[16] Yanda, H., Ghani, J. A., & Haron, C. H. C. (2010)," Effect of rake angle on stress, strain and temperature on the edge of carbide cutting tool in orthogonal cutting using FEM simulation,"ITB Journal of Engineering Science, 42 B(2), 179–194. https://doi.org/10.5614/itbj.eng.sci.2010.42.2.6

[17] Kisku, R. C. (2011)," Modelling of Temperature Profile in Turning With Uncoated and Coated Cemented Carbide Insert," National Institute of Technology, NIT Rourkela, Thesis, *107*.

[18] Saragi, E. (2012),"Modeling of temperature distribution in TRISO fuel-based on finite element method," AIP Conference Proceedings, 1448(3), 270–274. https://doi.org/10.1063/1.4725464

[19] . Y. R. B. (2013)," Finite Element Analysis on Temperature Distribution in Turning Process Using Deform-3D," International Journal of Research in Engineering and Technology, 02(06), 901–906. https://doi.org/10.15623/ijret.2013.020503

[20] Augustine, U., & Olisaemeka, N. (2013),” Thermal Aspect of Machining : Evaluation of Tool and Chip Temperature during Machining Process Using Numerical,” The International Journal Of Engineering And Science (IJES), 2(4), 66–79.

[21] Author, S. P. C. (2013),”Analytical Modeling of Temperature Distribution in Metal Cutting : Finite Element Approach ,” Onyechi , Pius C 1 ., Oluwadare , Benjamin S 2 ., Obuka , Nnaemeka. 2(4), 17–33. https://doi.org/10.15632/ijret.2014.0304147.CITATIONS

[22] KOHIR, V. V, & DUNDUR, S. T. (2014),”Finite Element Simulation to study the effect of flank wear land inclination on Cutting forces and temperature distribution in orthogonal machining,” The Journal of Engineering and Fundamentals, *1*(1), 30–42. https://doi.org/10.17530/jef.14.04.1.1

[23] Pervaiz, S., Deiab, I., Ibrahim, E. M., Rashid, A., & Nicolescua, M. (2014),”

A coupled FE and CFD approach to predict the cutting tool temperature profile in machining," Procedia CIRP, 17, 750–754. https://doi.org/10.1016/j.procir.2014.01.104

[24] Marcelo Ribeiro dos Santos,1 Sandro Metrevelle Marcondes de Lima e Silva, 2. (2014)," Analyses of effects of cutting parameters on cutting edge temperature using inverse heat conduction technique," Mathematical Problems in Engineering, 2014. https://doi.org/10.1155/2014/871859

[25] Steel, A. (2015)," Finite Element Machining Simulation of AISI6150 Steel,"November, 7959–7966. https://doi.org/10.15680/IJIRSET.2015.0408150

[26] Kumar, B. V. R. M., Hemachandra Reddy, K., & Vikram Kumar, C. R. (2016)," Finite element model based on abaqus / explicit to analyze the temperature effects of turning," International Journal of Applied Engineering Research, 11(8), 5728–5734.

[27] Kundrák, J., Gyáni, K., Tolvaj, B., Pálmai, Z., Tóth, R., & Markopoulos, A. P. (2017)," Thermotechnical modelling of hard turning: A computational fluid dynamics approach," Simulation Modelling Practice and Theory, 70, 52–64. https://doi.org/10.1016/j.simpat.2016.10.003

[28] Wang, B., Wang, L., & Zhang, E. (2017)," Finite element simulation of cutting grey iron HT250 by self-prepared Si3N4 ceramic insert," AIP Conference Proceedings, 1829(April). https://doi.org/10.1063/1.4979770

[29] Ojolo, S. J., Yinusa, A. A., & Ismail, S. O. (2017)," Modelling of temperature distribution in orthogonal machining sing finite element method," Advances in Transdisciplinary Engineering, 6, 427–432. https://doi.org/10.3233/978-1-61499-792-4-427

[30] Ferreira, D. C., Magalhães, E. dos S., Brito, R. F., & Lima E Silva, S. M. M.

(2018),” Numerical analysis of the influence of coatings on a cutting tool using COMSOL,” International Journal of Advanced Manufacturing Technology, 97(1–4), 1305–1314. https://doi.org/10.1007/s00170-018-1855-7

[31] Mohan Reddy, M., Kumar, M., & Shanmugam, K. (2018),” Finite element analysis and modeling of temperature distribution in turning of titanium alloys,” Metallurgical and Materials Engineering, 24(1), 59–69. https://doi.org/10.30544/323

[32] Akbar, A. A., Shwaish, R. R., & Hadi, N. D. (2018),” Study the Effect of Cutting Parameters on Temperature Distribution and Tool Life During Turning Stainless Steel 316L,” Al-Khwarizmi Engineering Journal, 14(3), 112–122. https://doi.org/10.22153/https://doi.org/10.22153/kej.2018.01.007

[33] Kanellos, P., Karkalos, N. E., & Markopoulos, A. P. (2019),” Numerical simulation of machining using a coupled FEM-CFD approach,” Procedia Manufacturing, 41, 795–802. https://doi.org/10.1016/j.promfg.2019.09.072

[34] Tu, L., Xu, F., Wang, X., Gao, J., Tian, S., Yuen, M. F., & Zuo, D. (2019),” Temperature distribution of cubic boron nitride–coated cutting tools by finite element analysis,” International Journal of Advanced Manufacturing Technology, 105(7–8), 3197–3207. https://doi.org/10.1007/s00170-019-04498-0

[35] Sahoo, S. (2019),” Review on Hard Turning using Finite Element Method,”Journal of Engineering Innovation and Research, 9(1), 61–68.

[36] Hussein, S. G., & Abdullah, M. Q. (2020),”Finite element analysis of heat flow and temperature distribution inside cutting tool,” Journal of Mechanical Engineering Research and Developments, 43(2), 406–414.

[37] Zhang, J., Meng, X., Du, J., Xiao, G., Chen, Z., Yi, M., & Xu, C. (2021),” Modelling and prediction of cutting temperature in the machining of h13 hard steel of transient heat conduction,” Materials, 14(12), 1–12.

https://doi.org/10.3390/ma14123176

[38] Guo, Y., Ye, W., & Xu, X. (2021),” Numerical and experimental investigation of the temperature rise of cutting tools caused by the tool deflection energy,” Machines, 9(6). https://doi.org/10.3390/machines9060122

[39] Mohammed, K. F. (2022),"Numerical study of heat transfer aspects in cutting tools made of Al 2 O 3 , ZrB 2 , TiB 2 , TiN using ANSYS fluent software ANSYS fluent yazılımı kullanılarak Al 2 O 3 , ZrB 2 , TiB 2 , TiN ’ den yapılmış kesici takımlarda ısı transferi yönlerinin sayısa," 11(1), 222–231. https://doi.org/10.28948/ngmuh.817836

[40] Outeiro, J. C., Dias, A. M., & Lebrun, J. L. (2004),” Experimental Assessment of Temperature Distribution in Three-Dimensional Cutting Process,” Machining Science and Technology, 8(3), 357–376. https://doi.org/10.1081/lmst-200038984

[41] Liljerehn, A., Kalhori, V., & Lundblad, M. (2009),” Experimental studies and modeling of heat generation in metal machining,” Machining Science and Technology, 13(4), 488–515. https://doi.org/10.1080/10910340903451506

[42] LB, A., & M, H. (2010),” Chip-Tool Interface Temperature Prediction Model for Turning Process,” International Journal of Engineering Science and Technology, 4(4), 382–393.

[43] B. Haddag • T. Kagnaya • M. Nouari • T. Cutar. (2013),” A new heat transfer analysis in machining based on two steps of 3D finite element modelling and experimental validation,” Heat and Mass Transfer/Waerme- Und Stoffuebertragung, 49(1), 129–145. https://doi.org/10.1007/s00231-012-1069-8

[44] Kulkarni, A. P., Joshi, G. G., Karekar, A., & Sargade, V. G. (2014),” Investigation on cutting temperature and cutting force in turning AISI 304 austenitic stainless steel using AlTiCrN coated carbide insert,” International Journal of Machining and Machinability of Materials, 15(3–4), 147–156. https://doi.org/10.1504/IJMMM.2014.060546

[45] Kato, T., & Fujii, H. (2014),"PVD Film Method for Measuring," Engineering for Industry, 1(February 1996), 1–6.

[46] Mzad, H. (2021)," Mathematical Simulation of Heat Generation at a Cutting-Tool Surface During Stock Removal Processes," Engineering Transactions, *69*(4), 423–436. https://doi.org/10.24423/EngTrans.1397.20211215

[47] Miller, L. (2020)," OpenCommons @ UConn A Thermal-Mechanical Finite Element Analysis of Orthogonal Cutting for Normalized Steels A Thermal-Mechanical Finite Element Analysis of Orthogonal Cutting for Normalized Steels," University of Connecticu.

[48] Haddag, B., Atlati, S., Nouari, M., & Zenasni, M. (2015)," Analysis of the heat transfer at the tool–workpiece interface in machining: determination of heat generation and heat transfer coefficients," Heat and Mass Transfer/Waerme-Und Stoffuebertragung, 51(10), 1355–1370. https://doi.org/10.1007/s00231-015-1499-1

[49] HK Versteeg and W Malalasekera, "An introduction to computational fluid dynamics", the finite volume method, first published, Longman groupLTD, 1996.

[50] Kadhim, A. M., Hassan, A. F., & Rishack, Q. A. (2021)," The Effect of Machining Parameters and Drill Point Angle on the Temperature Distribution in AISI 304 Stainless Steel During Dry Drilling Operation," 21(3), 25–33.

[51] Brito, R. F., Carvalho, S. R., & Silva, S. M. M. L. E. (2015)," Experimental Investigation of Thermal Aspects In A Cutting Tool Using Comsol And Inverse Problem," Applied Thermal Engineering, https://doi.org/10.1016/j.applthermaleng.2015.03.083

# الخلاصة

لتحسين إنتاجية عمليات التشغيل ، يجب معرفة توزيع درجات الحرارة في المشغولة وأداة القطع. معظم الطاقة المستخدمة لقطع المعدن أثناء عمليات القشط تتحول إلى حرارة. يتم تولد طاقة القص في ثلاث مناطق: المنطقة الأولية ، حيث يحدث التشوه البلاستيكي الرئيسي ، حيث منطقة اتصال الأداة مع الرايش. يحدث التشوه البلاستيك الثانوي بسبب الاحتكاك بين الرايش المسخن والأداة ، والمنطقة الثالثة ، حيث تتولد الحرارة في منطقة اتصال المشغولة واجهة أداة العمل. يتضمن ذلك توازن الحرارة بين الرايش والأداة الثابتة بالإضافة إلى طاقة الاحتكاك المتولدة في منطقة تلامس الرايش. تناولت هذه الرسالة تأثير متغيرات القطع على توزيع درجة الحرارة في عملية القشط وتم التحقيق عدديًا باستخدام طريقة Finite Element وطريقة Finite Volume استنادًا إلى برنامج ANSYS 2020R2. يتم تحديد درجة الحرارة في منطقة اتصال واجهة الأداة مع الرايش باستخدام Explicit Dynamic ، وهي تعتبر شروطًا حدودية في جانب واحد من الإدخال. تم عدديا دراسة تأثير انتقال وتدفق الحرارة على ادوات القطع والمصنوعة من صلب السرعات العالية، كاربيد و سيراميك بواسطة ANSYS FLUENT .تمت مقارنة الموديل العددي مع البحوث السابقة. وقد وجد توافقا جيدا جدا مع النتائج السابقة. يتكون نموذج المشغولة على شكل مستطيل بطول ، وارتفاع وعرض (150 مم) (50 مم) (30 مم) على التوالي. تم تحديد متغيرات القطع بثلاث سرعات (6 ، 8 ، 10) م / ث ، مع ثلاثة عمق قطع (1.5 ، 2 ، و 2.5) مم. بالنسبة لجميع عمليات المحاكاة ، فإن زاوية الجرف ثابتة (6)درجة. لقد اظهرت النتائج ، أن درجة الحرارة عند الحافة (منطقة التلامس بين قطعة العمل والأداة) كانت الأعلى وتنخفض تدريجياً باتجاه السطح ، وأن النتائج أظهرت تأثيرًا كبيرًا لسرعة القطع على درجة الحرارة المتولدة في الماكينة النماذج وتأثير صغير جدًا لعمق القطع على درجة حرارة قطعة العمل. وكذلك لقد أظهرت النتائج ان ادوات القطع المصنوعة من صلب السرعات العالية والكاربيد تمتلك حرارة اقل من تلك المصنوعة من السيراميك لذلك سوف تزداد انتاجية هذه الادوات. درجات الحرارة العظمى لصلب السرعات عالية كانت 537.14 K واما الكاربيد والسيراميك كانت 578.87 K, 648.3 K بتتابع. درجات الحرارة العظمى والصغرى كانت عند سرع قطع 6م/ث و 10 م/ث بتتابع. حالة القطع المثلى كانت عند استخدام صلب السرعات العالية كأداة قطع عند سرعة قطع 6 م/ث وعمق قطع 1.5 ملم.

جمهورية العراق

وزارة التعليم العالي والبحث العلمي

جامعة بابل/كلية الهندسة

قسم الهندسة الميكانيكية

# دراسة محاكاة توزيع درجة الحرارة على أداة القطع مع تأثير متغيرات عملية القطع

رسالة

مقدمة الى كلية الهندسة / جامعة بابل وهي جزء من متطلبات نيل شهادة الماجستير في الهندسة الميكانيكية /قدرة

اعدت من قبل

حنين حازم عبد العالي حسن

بأشراف

أ.م.د عبد الكريم جليل كاظم

و

أ.م.د سامر محمد عبد الحليم

1443م

2022م